UNIVERSITY OF TURKISH AERONAUTICAL ASSOCIATION
INSTITUTE OF SCIENCE AND TECHNOLOGY

EFFECTS OF DIFFERENT FIBRE ORIENTATIONS OF COMPOSITE MATERIALS ON THE PERFORMANCE OF ADHESIVELY BONDED JOINTS

MASTER THESIS

Hasan PÜSKÜL

Institute of Science and Technology

Mechanical And Aeronautical Engineering

FEBRUARY 2016

UNIVERSITY OF TURKISH AERONAUTICAL ASSOCIATION
INSTITUTE OF SCIENCE AND TECHNOLOGY

EFFECTS OF DIFFERENT FIBRE ORIENTATIONS OF COMPOSITE MATERIALS ON THE PERFORMANCE OF ADHESIVELY BONDED JOINTS

MASTER THESIS

Hasan PÜSKÜL

1303720006

Institute of Science and Technology

Mechanical and Aeronautical Engineering

Thesis Supervisor: Assoc. Prof. Dr. Ferhat KADIOĞLU

Türk Hava Kurumu Üniversitesi Fen Bilimleri Enstitüsü'nün 1303720006 numaralı Yüksek Lisans öğrencisi, "Hasan PÜSKÜL", ilgili yönetmeliklerin belirlediği gerekli tüm şartları yerine getirdikten sonra hazırladığı "KOMPOZİT MALZEMELERİN FARKLI ELYAF AÇILARININ YAPIŞTIRMA BAĞLAMA PERFORMANSINA ETKİLERİ (EFFECTS OF DIFFERENT FIBRE ORIENTATIONS OF COMPOSITE MATERIALS ON THE PERFORMANCE OF ADHESIVELY BONDED JOINTS)" başlıklı tezini, aşağıda imzaları olan jüri önünde başarı ile sunmuştur.

Tez Danışmanı : **Doç. Dr. Ferhat KADIOĞLU** ……………………

Jüri Üyeleri : **Doç. Dr. Ferhat KADIOĞLU** ……………………

: **Yrd. Doç. Dr. Munir ELFARRA**
Türk Hava Kurumu Üniversitesi ……………………

: **Yrd. Doç. Dr. Mustafa KAYA**
Türk Hava Kurumu Üniversitesi ……………………

Tez Savunma Tarihi: 26 Şubat 2016

UNIVERSITY OF TURKISH AERONAUTICAL ASSOCIATION
INSTITUTE OF SCIENCE AND TECHNOLOGY

Submitted by Hasan PÜSKÜL in partial fulfillment of the requirements for the degree of Master of Science in Mechanical and Aeronautical Engineering "EFFECTS OF DIFFERENT FIBRE ORIENTATIONS OF COMPOSITE MATERIALS ON THE PERFORMANCE OF ADHESIVELY BONDED JOINTS" I hereby declare that all information in this document has been obtained and presented in accordance with academic rules and ethical conduct. I also declare that, as required by these rules and conduct, I have fully cited and referenced all material and results that are not original to this work.

26.02.2016
Hasan PÜSKÜL

ACKNOWLEDGEMENTS

I would like to express my sincere gratitude to Assoc. Prof. Ferhat Kadıoğlu for his encouragement and supervision throughout my studies.

I would like to express my deepest gratitude to my wife Nimet, my son Hasan Utkan and my daughter Buğlem Nas for their loves.

I would like to thank to Assoc. Prof. Sinan Balcı and Assist. Prof. Tahsin Çağrı Şişman for offering suggestions and guidelines.

I would like to thank to Kılıç Ali Temiz and Cemal Şenyılmaz for their encouragement.

I would like to express my deep gratitude to my colleague Olcay Şenel, Hüseyin Ediz and Ziya Çevrim for their trust and encouragement.

I would like to special thank to Mustafa Kaplan and Uğur Ünal for their help to perform the experiments.

I would like to express deep gratitude to my colleague Türker Dölek for his help to produce the test parts.

I would like to thank to my friends Mahmut Yüksekyalçın, Ender Şaşal, Oğuz Kaan Baylak, Haşim Can, Fikret Cem Sönmez, Enes Erol, Ahmet Soner Koyuncu for their friendship.

Finally, I would like to thank to Dr. Yusuf Şimşek for his help.

February 2016 Hasan PÜSKÜL

TABLE OF CONTENT

ACKNOWLEDGEMENTS iv
TABLE OF CONTENT v
LIST OF TABLES viii
LIST OF FIGURES ix
ABBREVIATIONS xi
LIST OF SYMBOL xii
ABSTRACT xiii
ÖZET xv
CHAPTER ONE 1
1. INTRODUCTION 1
  1.1 Purpose 2
  1.2 Bolted Joints 2
    1.2.1 Advantages of Bolted Joints 3
    1.2.2 Disadvantages of Bolted Joints 3
  1.3 Adhesive Bonding 4
    1.3.1 Advantages of Adhesive Bonding 4
    1.3.2 Disadvantages of Adhesive Bonding 5
  1.4 Hybrid Joints 6
  1.5 Types of Curing 6
CHPATER TWO 8
2. COMPOSITE MATERIALS 8
  2.1 Advantages of Composite Materials on Aircraft Structural Parts 13
  2.2 Disadvantages of Composite Materials on Aircraft 15
  2.3 Glass Fiber 16
  2.4 Aramid Fibre (Kevlar®) 18
  2.5 Carbon Fibre 19
CHAPTER THREE 23
3. EXPERIMENTAL DATA 23
  3.1 Tool Preparation 23
    3.1.1 Tool 1 23

    - 3.1.2 Tool 2 24
- 3.2 Test Specimens 25
    - 3.2.1 Bending Test Specimen 29
    - 3.2.2 Bonding Test Specimen 29
- 3.3 Bonding Operation 30
    - 3.3.1 Preparation of Bonding Surface 30
    - 3.3.2 Application and Curing of Adhesive 31
- 3.4 Test Operations 32
- 3.5 The Three Point Bend Test Theory 32
- 3.6 Tensile Lap Shear Strength (Bond Strength Performance) Test Theory of Bonding 36

CHAPTER FOUR 37

4. RESULTS 37
- 4.1 Rectangular Three Point Bending Test Results 37
    - 4.1.1 0 Degree Samples 37
    - 4.1.2 15 Degree Samples 38
    - 4.1.3 30 Degree Samples 39
    - 4.1.4 45 Degree Samples 40
    - 4.1.5 60 Degree Samples 41
    - 4.1.6 75 Degree Samples 42
- 4.2 Tensile Lap Shear Strength of Single Lap Joint of Carbon 44
    - 4.2.1 Slj_c_0 44
    - 4.2.2 Slj_c_15 46
    - 4.2.3 Slj_c_30 48
    - 4.2.4 Slj_c_45 49
    - 4.2.5 Slj_c_60 52
    - 4.2.6 Slj_c_75 53
        - 4.2.6.1 Slj_c_75_I 54
        - 4.2.6.2 Slj_c_75_II 54
        - 4.2.6.3 Slj_c_75_III 54
        - 4.2.6.4 Slj_c_75_IV 54
        - 4.2.6.5 Slj_c_75_V 54
- 4.3 Flexural Strength (σ) of Carbon Fibres 55

CHAPTER FIVE 57

5. DISCUSSION 57

CHAPTER SIX 60

6. CONCLUSION 60

REFERENCES 61
Appendix-A: Ply Orientation Tables are Given Below For Each Test Specimen 66
Appendix-B: In This Section, Detailed Calculations of 0 Degree Sample is Given 70
Appendix-C: Here, Detailed Calculations Of Tensile Lap Shear Strength of Single Lap Joints of Carbon Fibre are Given 72
RESUME 73

LIST OF TABLES

Table 3.1 : Autoclave report. 27
Table 3.2 : Material type and cleaning method. 30
Table 4.1 : Young’s Modulus of 0 degree samples. 38
Table 4.2 : Young’s Modulus of 15 degree samples. 39
Table 4.3 : Young’s Modulus of 30 degree samples. 40
Table 4.4 : Young’s modulus of 45 degree samples. 41
Table 4.5 : Young’s Modulus of 60 degree samples. 42
Table 4.6 : Young’s Modulus of 75 degree samples. 43
Table 4.7 : Tensile lap shear strength of 0 degree samples. 45
Table 4.8 : Tensile lap shear strength of 15 degree samples. 47
Table 4.9 : Tensile lap shear strength of 30 degree samples. 49
Table 4.10 : Tensile lap shear strength of 45 degree samples. 51
Table 4.11 : Tensile lap shear strength of 60 degree samples. 53

LIST OF FIGURES

Figure 1.1 : Bolted joint. 1
Figure 1.2 : Bolt and adhesive together. 2
Figure 1.3 : Single lap joint assembly. 2
Figure 1.4 : Double lap joint. 2
Figure 1.5 : Types of curing. 7
Figure 2.1 : Major composite parts of A380 9
Figure 2.2 : Matrices. 10
Figure 2.3 : Reinforcements. 11
Figure 2.4 : Thermosets. 12
Figure 2.5 : Composite materials. 13
Figure 2.6 : Glass fiber. Taken from 16
Figure 2.7 : Schematic of manufacturing glass fiber form. Adapted from 17
Figure 2.8 : Aramid fiber. Taken from 18
Figure 2.9 : Aromatic compound of aramid fiber. Taken from 19
Figure 2.10 : Graphite fiber. Taken from 19
Figure 2.11 : Manufacturing of graphite fibers. Taken from 21
Figure 3.1 : Technical drawing of tool 1. 23
Figure 3.2 : Technical drawing of part 1 of tool 2. 24
Figure 3.3 : Technical drawing of part 2 of tool 2. 25
Figure 3.4 : Curing information. 28
Figure 3.5 : Parts after curing. 29
Figure 3.6 : 0 degree test sample for bending. 29
Figure 3.7 : 0 degree test sample for bonding. 29
Figure 3.8 : Personal protective equipments. 30
Figure 3.9 : Abrasive paper. Taken from [49]. 31
Figure 3.10 : Bond area. 31
Figure 3.11 : Metal parts used for adjusting the thickness of adhesive. 32
Figure 3.12 : Alignment of metal parts. 32
Figure 3.13 : Tensile and compressive forces. Adapted from 33
Figure 3.14 : The three point bending test set-up. Taken from 33
Figure 3.15 : Rectangular three point bending test. Adapted from 33
Figure 3.16 : Apparatus of shear test of bonded material. 36
Figure 4.1 : Graphical representation of bnd_0 results. 38
Figure 4.2 : Graphical representation of bnd_15 results. 39
Figure 4.3 : Graphical representation of bnd_30 results. 40
Figure 4.4 : Graphical representation of bnd_45 results. 41
Figure 4.5 : Graphical representation of bnd_60 results. 42
Figure 4.6 : Graphical representation of bnd_75 results. 43
Figure 4.7 : Graphic representation of load vs. displacement. 44
Figure 4.8 : Test sample of slj_c_0_I. 45
Figure 4.9 : Bonded area of test sample. 45

Figure 4.10 : Graphical representation of slj_c_0 results. 46
Figure 4.11 : Test sample of slj_c_15_I and slj_c_15_II. 46
Figure 4.12 : Bonded surface deformation after adhesive break. 47
Figure 4.13 : Graphical representation of slj_c_15 results. 47
Figure 4.14 : Test sample of slj_c_30_I and slj_c_30_II. 48
Figure 4.15 : View of test part after breaking. 48
Figure 4.16 : Graphical representation of slj_c_30 results. 49
Figure 4.17 : Test sample of slj_c_45_I, II and III. 50
Figure 4.18 : Breaking away part in the bonded area. 50
Figure 4.19 : Graphical representation of slj_c_45 results. 51
Figure 4.20 : Test sample of slj_c_60_I, II, III and IV. 52
Figure 4.21 : Graphical representation of slj_c_60 results. 53
Figure 4.22 : Test sample of slj_c_75_I and II. 54
Figure 4.23 : Graphical representation of slj_c_75 results. 55
Figure 4.24 : Graphic representation of load vs. displacement of shear test. 55
Figure 4.25 : Graphic representation of load vs. angle orientation of carbon fiber. 56

ABBREVIATIONS

CMC : Ceramic Matrix Composites
FRC : Fiber Reinforced Composites
MMC : Metal Matrix Composites
OMC : Organic Matrix Composites
PAN : Poly-Acrylo-Nitrile
PMC : Polymer Matrix Composites
PPE : Personel Protective Equipments
UD : Unidirectional

LIST OF SYMBOL

E : modulus of elasticity (Young’s modulus), (in Pa)
δ : displacement, (in m)
σ : flexural strength, (in Pa)
τ : tensile lap shear strength, (in Pa)
M : moment, (in Nm)
I : polar moment of inertia, (in m^4)
F : force, (in N)
L : length of support, (in m)
b : wide, (in m)
h : height, (in m)
y : distance from the center of the specimen to the convex surface, (in m)

ABSTRACT

EFFECTS OF DIFFERENT FIBRE ORIENTATIONS OF COMPOSITE MATERIALS ON THE PERFORMANCE OF ADHESIVELY BONDED JOINTS

PÜSKÜL, Hasan
Master, M.S. in Mechanical and Aeronautical Engineering
Supervisor: Assoc. Prof. Ferhat KADIOĞLU
February 2016, 73 pages

The increased use of adhesively joined structural composite parts in aerospace and aircraft demand a thorough understanding of their behavior under loads. The strength of adhesively bonded joints depend on several factors such as joint geometry, adhesive type, adhesive thickness, adherent properties, loading directions and loading conditions.

In this thesis study, effects of different fibre orientations of composite materials on the performance of adhesively bonded joints have been examined. Fibre orientations are considered in 0, 15, 30, 45, 60 and 75 degrees. Each part of the sample includes 12 plies. Plies have been placed cross to each other except for 0 degree. For example, first ply has been placed +15 and second ply has been placed -15 degree. The following plies have been placed $(+15/-15)_2$. At the midpoint, sixth and seventh plies have been placed in the same degree. Mechanical properties of carbon fibre composite materials with different orientations have been examined in a single lap joint. Additionally, these parts have been subjected to the three point bending test. These parts produced from carbon material are unidirectional fibres. The adhesive used to bond parts is Hysol® EA9394, two-part adhesive. Results revealed that mechanical properties of the lap joint are influenced by the adherent fibre orientation. The strength of bonded joints of parts produced with the orientation of fibres at 0 degree was higher than that of 15 degree. As expected, the strength of bonded joints of parts produced with the orientation of fibres 15 degree was higher than that of 30 degree. And similarly, the strength of other orientations was decreasing as the angle of orientation increased. At 75 degree, the sample has been broken down. On the bonded area, no deformation was observed.

In the bending test, we have calculated the elasticity modulus (Young's modulus) of the sample. We determined that samples produced at 0 degree angle orientation have the highest elasticity modulus. As the angle orientations are getting further from 0, elasticity modulus are drastically decreasing. 75 degree samples showed the lowest elasticity modulus.

The result of this study revealed that the orientation of fibre should be considered while designing lap joints.

Keywords: adhesive bonding, bonding strength, bolted joint, composite materials, lap joint, and tensile strength.

ÖZET

KOMPOZİT MALZEMELERİN FARKLI ELYAF AÇILARININ YAPIŞTIRMA BAĞLAMA PERFORMANSINA ETKİLERİ

PÜSKÜL, Hasan
Yüksek Lisans Tezi, Makine ve Uçak Mühendisliği Anabilim Dalı
Tez Danışmanı: Doç. Dr. Ferhat KADIOĞLU
Şubat 2016, 73 sayfa

Havacılık ve uzay sanayisinde yapıştırıcı ile yapıştırılarak birleştirilen yapısal parçaların kullanımı her geçen gün artması kompozit parçaların yük altındaki davranışlarını derinlemesine anlamaktan geçer. Yapısal yapıştırmanın mukavemeti birleşme geometrisine, yapıştırıcı çeşidine, yapıştırıcı kalınlığına, yapışan parçaların özelliklerine ve yükün yönüne ve koşullarına bağlıdır.

Bu çalışmada Kompozit malzemelerin farklı elyaf açılarının yapıştırma bağlama performansına etkileri incelenmiştir. Elyaf açıları olarak 0 derece, 15 derece, 30 derece, 45 derece, 60 derece ve 75 derece kullanılmıştır. Her bir parça 12 katmandan oluşmaktadır. Katmanlar, 0 derece hariç, çapraz olarak yerleştirilmiştir. Örnek, ilk elyaf +15 yönünde serilmiş ise ikinci elyaf -15 yönünde serilmiştir. Orta noktada altıncı ve yedinci katmanlar aynı yönde serilmiştir. Karbon kompozit yapıların farklı açılarda tek bindirmeli birleştirmenin mekanik özellikleri değerlendirilmiştir. Aynı zamanda bu parçalar üç noktalı eğme testine tabi tutulmuştur. Kullanılan karbon elyaflar tek yönlüdür. Parçaları yapıştırmak için kullanılan yapıştırıcı iki parçalı Hysol EA9394’dür. Bu çalışmanın sonuçları göstermiştir ki tek bindirmeli yapıştırma birleştirmeleri elyaf açılarından etkilenmektedir. Yapıştırmanın kuvveti 0 dereceden üretilmiş parçalarda en fazla değeri sahiptir. Beklendiği gibi açı değeri arttıkça yapıştırma kuvveti de azalmaktadır. En fazla kuvvet 0 derecede iken 75 derecen üretilen parçalar teste tabi tutulduğunda parça kırılmıştır. Yapışma bölgesinde herhangi bir hasar gözlenmemiştir.

Eğme testinde elastik modül değeri (Young’s Modulus) hesaplanmıştır. 0 derece en yüksek elastik değerine, 75 derecenin ise en az değere sahip olduğu görülmüştür.

Bu çalışmanın sonuçları göstermiştir ki tek bindirmeli birleştirmelerin tasarımında elyaf açıları mutlaka dikkate alınmalıdır.

Anahtar kelimeler: cıvata ile birleştirme, çekme mukavemeti, karma malzemeler, tek bindirmeli birleştirme, yapışma kuvveti, yapıştırma

CHAPTER ONE

INTRODUCTION

The main problem in aerospace structural parts is joining of these parts together. Since there are many external affects that the joining technique must resist. In joining process, several methods are used. In addition, the joining technique must be so simple, reliable and cheap [1]. With the appropriate joining technique it should be possible to transmit loads safely into joining part. This can be achieved with a suitable joining technique. Designing joints in the context of fibre reinforcement plastics is usually too complex, independently from the considered type of joint [2].

Bolted joint (Fig. 1.1), bonding of parts and using of both bolt and adhesive together (Fig. 1.2) are just examples of these methods. There are also types of bonding according to assembly, single lap joint (Fig. 1.3), double lap joint (Fig. 1.4), etc. and also we can divide the bonding according to types of material that bonded together, composite bonding, metal bonding, hybrid bonding, etc. In bonding process there are parts and adhesive, in bolted process there are bolt-nut and parts.

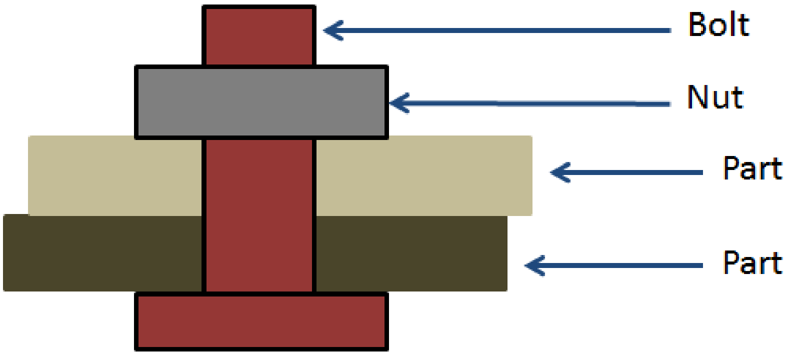

Figure 1.1: Bolted joint.

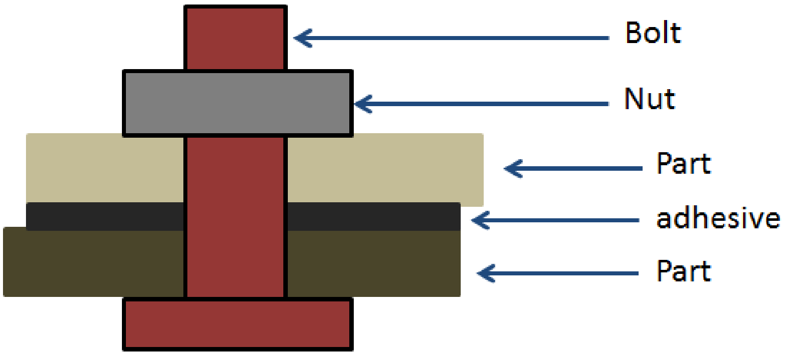

Figure 1.2: Bolt and adhesive together.

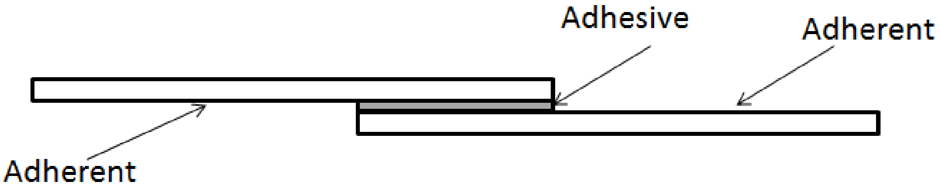

Figure 1.3: Single lap joint assembly.

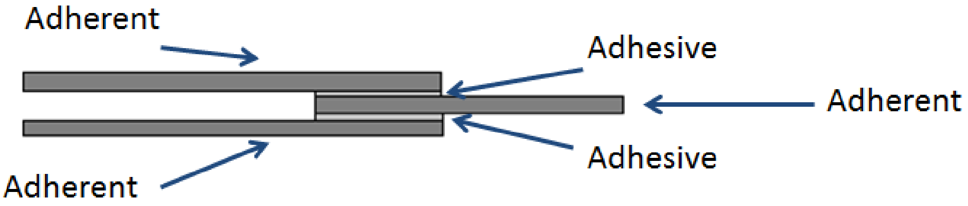

Figure 1.4: Double lap joint.

1.1 Purpose

The aim of this thesis study is to present effects of fiber orientations for bonding strength. We are dealing with unidirectional (UD) carbon-epoxy material parts bonded with two-part adhesive as single lap joint.

1.2 Bolted Joints

Bolted joints are one of the most common connection types in structure assemblies. They consist of fasteners that capture and join other parts together, and are secured with the mating of screw threads nuts, but the joining technique needs a specific torque value to capture the parts. Some accurate and useful papers dealing with the mechanical behavior of mechanically fastened joints are available in the literature [3-5].

There are two main types of bolted joint designs: tension joints and shear joints.

In the tension joint, the bolt-nut and clamped components of the joint are designed to transfer the external tension load through the joint by the way of the clamped components through the design of a proper balance of joint and bolt stiffness. The joint should be designed such that the clamp load is never overcome by the external tension forces acting to separate the joint.

The second type of bolted joint, which is shear joint, transfers the applied load in shear on the bolt shank and relies on the shear strength of the bolt. Tension loads on such a joint are only incidental. A preload is still applied but is not as critical as in the case where loads are transmitted through the joint in tension. Other such shear joints do not employ a preload on the bolt as they allow rotation of the joint about the bolt, but use other methods of maintaining bolted joint integrity. This may include clevis linkages, movable joints, and joints that rely on a locking mechanism (like lock washers, thread adhesives, and lock nuts).

Proper joint design and bolt preload provide useful mechanical properties. Chen has stated in his work that the pull-through strength was found to be influenced by laminate thickness, stacking sequence, resin system, laminate size, fastener head diameter and environmental condition and friction [6].

Countersink type of fastener is used by Stocchi et al. in their work to investigate the effect of the coefficient of friction, clamping force and clearance on the joint behavior [7].

1.2.1 Advantages of Bolted Joints

There are some advantages of bolted joints.

a) Disassembled. Bolted joints can be easily disassembled and assembled.
b) Inspection. Simple and cheap inspection procedure.
c) Not environmentally sensitive.

1.2.2 Disadvantages of Bolted Joints

There are some disadvantages of bolted joints.

a) Corrosion. Prone to corrosion in metal parts.

b) Filler material. Bolted joints may require extensive shimming for assembly.
c) Stress. Considerable stress concentration on joints.
d) Fatigue. Prone to fatigue cracking in metallic component in life time.

1.3 Adhesive Bonding

There is a basic rule for achieving the highest strength during bringing parts together, use bonding for thin laminates and bolting for thick laminates. The thickness of parts refers to the original laminate or skin, excluding any core materials. Adhesive bonding describes a layer bonding technique with applying an intermediate layer to connect the substrates of different materials.

Adhesive bonding technique is increasingly used nowadays in aeronautical and other industries for its convenience and high efficiency [8]. Adhesive bonding technique has been studied some researchers in recent decades. Jianfeng Li at al. [8] has experimentally studied the adhesively bonded carbon fibre reinforced plastics (CFRP) subjected to tensile loads. Banea and da Silva et al. [9, 10] stated a very simple comprehensive review on the bond strength and analytical models of adhesively bonded CFRP joints.

Adhesive bonding is the surface-to-surface joining of similar or dissimilar materials using a different type of substance, and which adheres to the surfaces of the two adherents to be joined, transferring the forces from one adherent to the other [11]. Adhesive bonding is a material joining technique that cannot be broken without destruction of the bond area and sometimes the adherents can be damaged.

1.3.1 Advantages of Adhesive Bonding

There are some advantages of bonding:

a) Stress-bearing. Bonding provides large stress-bearing area
b) Good barrier. So important, minimize or prevent galvanic corrosion between dissimilar materials.
c) Thickness. Join all shapes and thicknesses
d) Different materials. Join any combination of similar or dissimilar materials.
e) Seal all joint area on the part.

f) Generally less expensive and faster than mechanical fastening
g) Provide us attractive strength to weight ratio.
h) Reduce the noise and vibration because of filling the bond area.
i) Reduce the number of components such as screws, nuts, washers, bolts, securing equipment…
j) Conductive. Some special adhesives there are to conduct electricity.
k) Faster and cheaper joining technique
l) Provide us thin and invisible joint area.
m) Joints sometimes may be electrically/thermally conductive or insulating.
n) Uniform distribution. Mechanical stress over the joint is distributed uniformly.
o) No leakage. Gas-proof and liquid-tight.

1.3.2 Disadvantages of Adhesive Bonding

There are some disadvantages of adhesive bonding:

a) Main point is cleaning of bonding surfaces of substrates. Surfaces must be cleaned carefully with appropriate cleaner.
b) Generally heat and pressure may be needed to cure the adhesive.
c) Inspection of bonding area is difficult or too expensive. R. A. Pethrick has stated the use of high-frequency dielectric measurements for the non-destructive evaluation of adhesively bonded structures [12]. David K. HSU has described the nondestructive inspection methods of composite structures [13].
d) Jigs and fixture may be needed to bond.
e) Heat sensitive parts could not bond. The temperature of using condition.
f) Takes too much time to cure. Fast cure is available.
g) Maintenance. Removal or disassembly of components can destroy the parts that joint together
h) The basis of the adhesives is chemical compounds, for this reason it is necessary to define the needed actions to prevent human exposure to these products during the time of application.
i) Limits to thickness that can be joined with simple joint configuration
j) Prone to environmental effects. Environmentally sensitive.

k) Usage condition. Service temperature and environment limitation.
l) Mixing. Mixing ratio is so important.
m) Pot life. Time limitation to apply adhesive.
n) The basis of the adhesives is chemical compounds, for this reason shelf life is important.

1.4 Hybrid Joints

In this type of joint, both bolt and adhesive are used together to resist the forces and loads. While the bolts keep the parts together, adhesive distributes the loads homogenously over the bolts. It is conceptually possible to combine both, and achieve a combined bolted/bonded connection, which research refers to as ‘‘hybrid’’ [14-15]. And also Kobye Bodjona and Larry Lessard have defined a possible alternative that has recently garnered interest consists of combining bonding and bolting in what is known as a bonded/bolted joint or a hybrid joint [16]. Till Vallee et al. have stated that the concept of combining bolts with an adhesive layer seems elegant; for example mechanical fasteners might be considered as back-up system for a failing adhesive layer [2].

A number of studies have shown that bonded/bolted joints know as hybrid joints can potentially achieve greater static strength and fatigue strength than the underlying bonded and bolted joints separately [17-20].

Hybrid joints show the advantages of both adhesive and bolt together, while show some disadvantages of both such as resist to temperature, inspection.

1.5 Types of Curing

There are three main concepts to prepare the joints with adhesive. These are co-curing, co-bonding and secondary bonding (Fig. 1.5). In the co-curing process two parts are simultaneously cured. The interface between the two parts may or may not have an adhesive layer since the resin is uncured. A typical co-curing application in aerospace is the simultaneous cure of a stiffener and a skin. Adhesive film a kind of adhesive is frequently placed into the interface between the stiffener and the skin to increase fatigue and peel resistance. Principal advantages derived from the co-curing process are excellent fit between bonded components and guaranteed surface cleanliness [21]. Parts must be cured in autoclave.

In the co-bonding process, one of the detail parts was cured before with the mating part being cured simultaneously with the adhesive. Since one of the parts was cured in this case adhesive shall be used. Film adhesive is often used to improve peel strength. Honeycomb sandwich assemblies generally use co- bonding process to ensure optimal structural performance. Also for this process parts must be cured in autoclave.

In the last bonding process, secondary bonding, bonding utilizes precured composite detail parts, and uses a layer of adhesive to bond two precured composite parts. In this case parts can be cured in autoclave or not. Depending up on the adhesive cure can be done outside the autoclave.

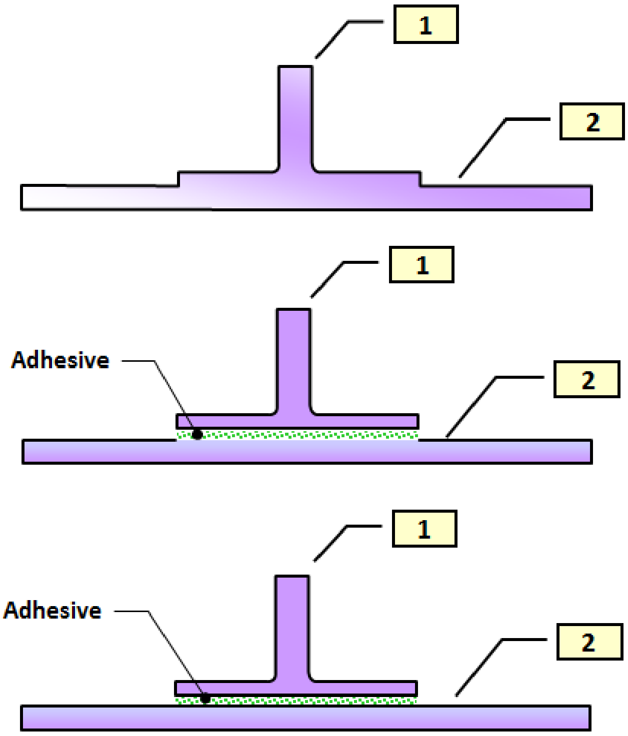

Figure 1.5: Types of curing.

CHPATER TWO

COMPOSITE MATERIALS

Structural materials can be divided into four basic categories: metals, polymers, ceramics and composites. Composites, which consist of two or more separate materials combined in a macroscopic structural unit, are made from various combinations of the other metals, polymers and ceramics [22].

Nowadays, composite materials become more and more important in the construction of primary aerospace structures, especially for aircrafts. In figure 2.1, the newest aircraft of Airbus A380 is shown, it is easily seen that the percentage of composite materials used on aircraft [23]. Since Wright Brothers built their Flyer back in 1903, the materials used in airplane design have been constantly evolving. For example, Boeing 747 type aircraft, built in 1969, has composite parts a percentage of 11% over the full aircraft. In Boeing 787 type aircraft, the ratio of composite materials is drastically increased to over 50%. The original Wright Flyer was comprised primarily of spruce and ash wood with muslin covering the wings. Today aircrafts are mostly made of aluminum with some structure made from steel. In the mid 1960's, scientists and engineers began working for new aerospace materials called composites. A composite is an engineered material made from two or more components showing significantly different mechanical properties, either physical or chemical [24]. While no longer used today, an early example of a composite material is a mixture of mud and straw that is used to make bricks.

A composite material is a structural material, which consists of two or more combined constituents, which are combined at a macroscopic level and are not soluble in each other [25]. One constituent is called the reinforcing element and the other one in which it is embedded is called the matrix element.

Advanced composites materials are defined as composite materials that are generally used in the aerospace applications.

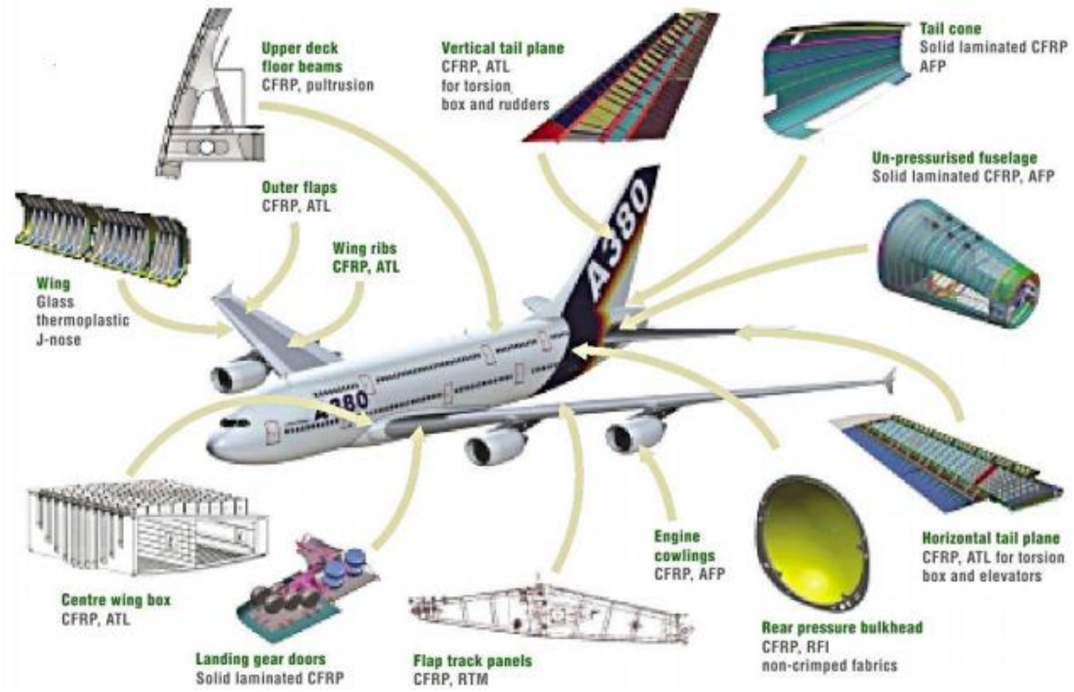

Figure 2.1: Major composite parts of A380 [24].

Aircraft parts made from composite materials, such as fairings, wings, radome, spoilers, and flight controls, were developed during the 1960s for their weight savings and strengthens over aluminum parts [21]. New generation large aircrafts are designed with all composite fuselage and wing structures using different production methods such as fibre placement. As a result of this, the repair of these composite materials requires an in-depth knowledge of composite structures, materials and tooling.

Composite materials are commonly classified at following two distinct levels according to constituent [26].

a) The first level of classification is usually made with respect to the matrix constituent (Fig. 2.2). The major composite classes include Organic Matrix Composites (OMCs), Metal Matrix Composites (MMCs) and Ceramic Matrix Composites (CMCs). The term organic matrix composite is generally assumed to include two classes of composites, namely Polymer Matrix Composites (PMCs) and carbon matrix composites commonly referred to as carbon-carbon composites.

Polymer Matrix Composites can be further divided into two groups, one is thermoset the other is thermoplastic.

b) The second level of classification refers to the reinforcement form (Fig. 2.3): fiber reinforced composites, laminar composites and particulate composites. Fiber reinforced composites can be further divided into those containing discontinuous fibers or continuous fibers.

Fiber reinforced composites (FRC) are composed of fibers embedded in matrix material, resin. Such a composite is considered to be a discontinuous fiber or short fiber composite if its properties vary with fiber length or strength depends on fiber length. On the other hand, when the length of the fiber is such that any further increase in length does not further increase, the elastic modulus of the composite, the composite is considered to be continuous fiber reinforced. Fibers are small in diameter and when pushed axially, they bend easily although they have very good tensile properties. These fibers must be supported to keep individual fibers from bending and buckling.

Laminar Composites are composed of layers of materials held together by matrix. Sandwich structures fall under this category.

Particulate Composites are composed of particles distributed or embedded in a matrix body. The particles may be flakes or in powder form or whiskers form. Concrete and wood particle boards are examples of this category.

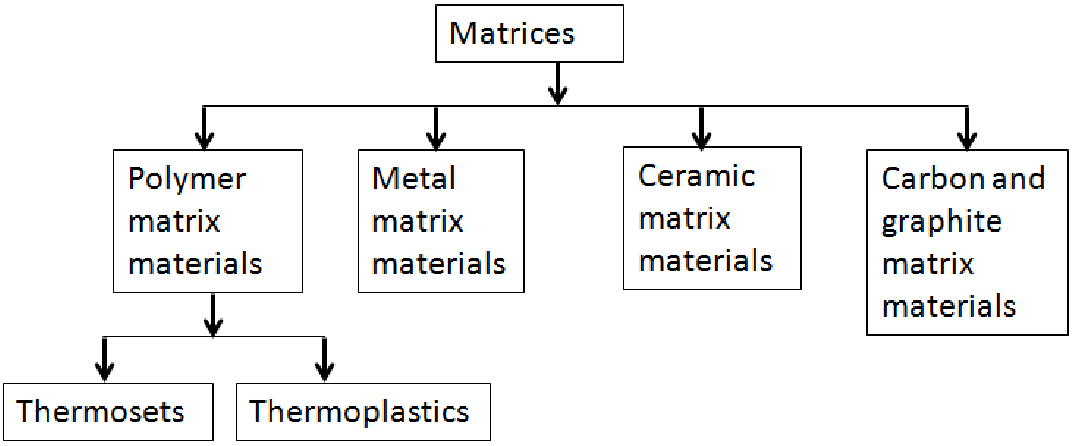

Figure 2.2: Matrices.

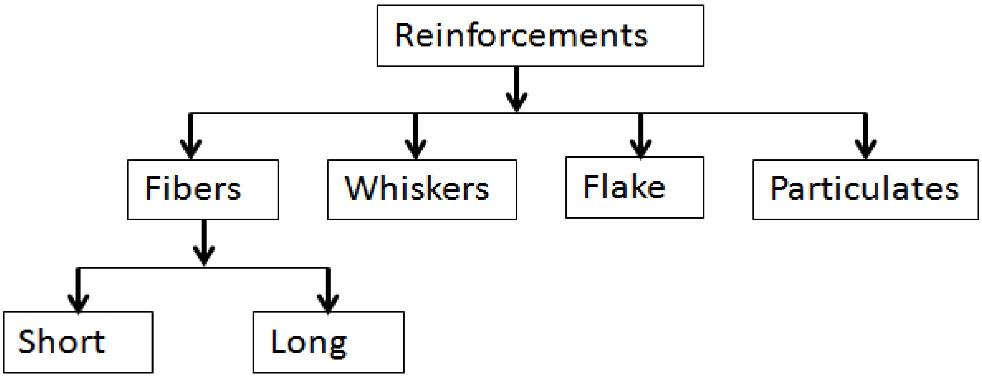

Figure 2.3: Reinforcements.

It is exactly true that the high strength of composites is largely due to the fiber reinforcement, the importance of matrix material cannot be ignored as it provides support for the fibers and assists the fibers in carrying the loads. It also provides stability to the composite material. Resin matrix system acts as a binding agent in a structural component in which the fibers are embedded. When too much resin is used, the part is classified as resin rich. On the other hand if there is too little resin, the part is called resin starved or fiber rich. A resin rich part is more susceptible to cracking due to lack of fiber support, whereas a resin starved part is weaker because of void areas and the fact that fibers are not held together and they are not well supported. So mixing ratio of fiber and resin is very important. Function of matrix/resin in composite parts is described as follows:

a) Holds the fibers together in the structure.
b) Protects the fibers from environmental effects, such as rain, humid...
c) Distributes loads equally between fibers so that all fibers are subjected to the same amount of strain.
d) Enhances transverse properties of a laminate.
e) Improves fracture and impact resistance of a component.
f) Helps to avoid propagation of crack growth through the fibers by providing alternate failure path along the interface between the fibers and the matrix.
g) Carry interlaminar shear.

Polymers are ideal materials when they are processed easily, and they are lightweight and have desirable mechanical properties [26]. High temperature matrix/resins are extensively used in aeronautical applications.

There are two main types of polymers, which are thermosets and thermoplastics. Thermosets have useful qualities such as a well-bonded threedimensional molecular structure after curing. Their decompositions are irreversible. Only changing the basic composition ratio of the resin is enough to alter conditions suitably for curing and determining its other mechanical properties. Thermosets have a wide range of applications in the chopped fiber composites form particularly when a premixed or moulding compound with fibers of specific quality and aspect ratio happens to be starting material as in epoxy, polymer and phenolic polyamide resins.

Thermoplastics have one- or two-dimensional molecular structure and they tend to act an elevated temperature and show exaggerated melting point. Another advantage of thermoplastics is that the process of softening at elevated temperatures can be reversible to regain its properties during cooling, facilitating applications of conventional compress techniques to mould the compounds.

Thermosets are the most popular of the fiber composite matrices used in industry especially aircraft application. Aerospace components, automobile parts, defense systems etc., use a great deal of this type of fiber composites. There are some types of thermosets (Fig. 2.4), epoxy, polyester, polyamide, phenolic, etc.

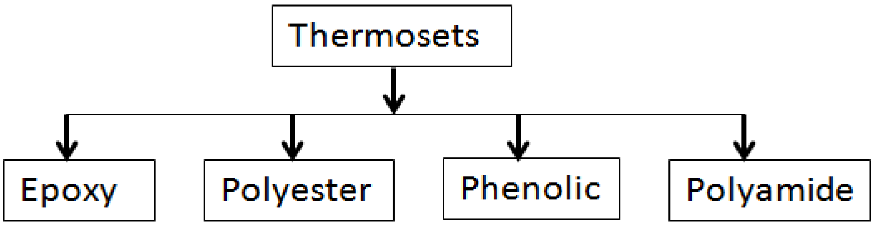

Figure 2.4: Thermosets.

The most widely used matrices for composites used in aircraft industry are epoxy resins. These resins cost more than polyesters and do not show durability at high temperature applications. But bismaleimides or polyamides show durability at high temperature. Epoxy resins are also widely used in filament-winding composites and preimpregnated (prepreg) applications. Moreover, they are suitable for moulding applications. Some advantages of epoxy resin listed as:

a) Stable to chemical attacks and solvents,
b) Excellent adherents having slow and low shrinkage during curing,
c) No emission of volatile gases,
d) Good electrical properties,
e) Adjustable curing rate,

f) Good adhesion to fiber and to resin,

g) Wide range of curative options.

These advantages, however, make the usage of epoxies rather expensive from other thermosets, except bismaleimides. They cannot be used such applications above a temperature of 100ºC. Their usage in high technology areas where service temperatures are higher is limited.

Composites materials are comprised of fibre reinforcements that bonded together with a matrix (Fig. 2.5) material [27]. In our composite samples, we used epoxy resins.

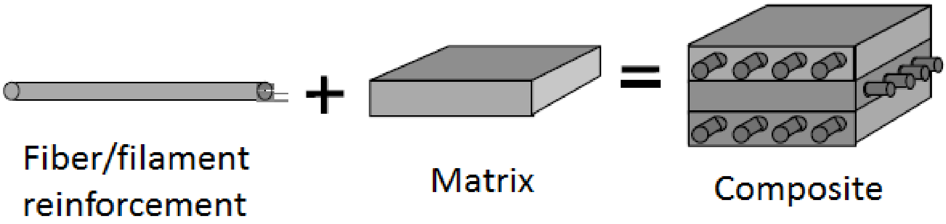

Figure 2.5: Composite materials.

Composite material usage shows increasing trends in aircraft industries. We can list many advantages of composite materials. Additionally, we can present many disadvantages of composite materials for the reason of an aircraft that are not made from composite materials totally.

2.1 Advantages of Composite Materials on Aircraft Structural Parts

There are some advantages of composites parts

a) High resistance to fatigue and corrosion degradation

b) High strength or stiffness to weight ratio. Lighter aircraft means more loads to be carried, more fuel to go further.

c) Due to greater reliability, there are fewer inspections and structural repairs.

d) Directional tailoring capabilities to meet the design requirements. The fiber pattern can be laid in a manner that will tailor the structure to efficiently sustain the applied loads.

e) Fiber to fiber redundant load path.

f) It is easier to achieve smooth aerodynamic profiles for drag reduction. Complex double-curvature parts with a smooth surface finish can be made in one manufacturing operation.

g) Composites offer improved torsional stiffness. This implies high whirling speeds, reduced number of intermediate bearings and supporting structural elements. The overall part count and manufacturing and assembly costs are thus reduced.

h) High resistance to impact damage.

i) Thermoplastics have rapid process cycles, making them attractive for high volume commercial applications that traditionally have been the domain of sheet metals. Moreover, thermoplastics can also be reformed.

j) Like metals, thermoplastics have indefinite shelf life.

k) Composites are dimensionally stable i.e. they have low thermal conductivity and low coefficient of thermal expansion. Composite materials can be tailored to comply with a broad range of thermal expansion design requirements and to minimize thermal stresses.

l) Manufacturing and assembly are simplified because of part integration (joint/fastener reduction) thereby reducing cost and time.

m) The improved weatherability of composites in a marine environment as well as their corrosion resistance and durability reduce the down time for maintenance.

n) Close tolerances can be achieved without machining.

o) Material is reduced because composite parts and structures are frequently built to shape rather than machined to the required configuration, as is common with metals.

p) Excellent heat sink properties of composites, especially Carbon-Carbon, combined with their lightweight have extended their use for aircraft brakes.

q) Improved friction and wear properties.

r) The ability to tailor the basic material properties of a Laminate has allowed new approaches to the design of aeroelastic flight structures.

2.2 Disadvantages of Composite Materials on Aircraft

There are some disadvantages of composite parts.

a) High cost of raw materials and fabrication.
b) Composites are more brittle than wrought metals and thus are more easily damaged.
c) Transverse properties may be weak.
d) Matrix is weak, therefore, low toughness.
e) Reuse and disposal may be difficult.
f) Difficult to attach.
g) Repair introduces new problems, for the following reasons:
   1. Materials require refrigerated transport and storage and have limited shelf life.
   2. Hot curing is necessary in many cases and requiring special tooling.
   3. Hot or cold curing takes time.
   4. Hot or wet methods need different tooling.
h) Analysis is difficult.
i) Matrix is subject to environmental degradation. Environmental effects on composite structure have been studied by some researchers [28-32]
j) Storage condition and control of storage condition are so strict.
k) Shelf life is limited.

However, proper design and material selection can circumvent many of the above disadvantages. New technology has provided a variety of reinforcing fibers and matrices those can be combined to form composites having a wide range of exceptional properties. Since the advanced composites are capable of providing structural efficiency at lower weights as compared to equivalent metallic structures, they have emerged as the primary materials for future use.

In aircraft application, advanced fiber reinforced composites are now being used in many structural applications, floor beams, engine cowlings, flight control surfaces, landing gear doors, wing-to-body fairings, etc., and also major load carrying structures including the vertical and horizontal stabilizer main torque boxes. For an aircraft glass fiber, aramid and carbon fiber are commonly used materials.

2.3 Glass Fiber

Glass fibers (Fig. 2.6) are one of the most versatile industrial materials known today [33]. They are easily produced from raw materials, which are abundant in the world [34].

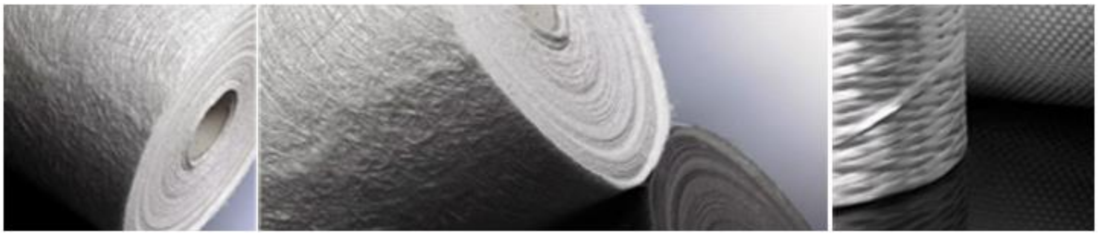

Figure 2.6: Glass fiber. Taken from [35].

Glass fiber reinforced polymer matrix composites are the most popular reinforced plastic materials used in construction industry. Depending upon the formation and usage, they may be fabricated into products that are lightweight, transparent or opaque, colorless or colored, flat or shaped sheets, with any size of object can be made [36].

Glass fibers are produced generally via drawing from a melt as shown in Figure 2.7. The melt is formed in a refractory furnace at about 2550°F (1400°C) from a mixture that includes sand, limestone, and alumina. Then, the melt is stirred and maintained at a constant temperature [25].

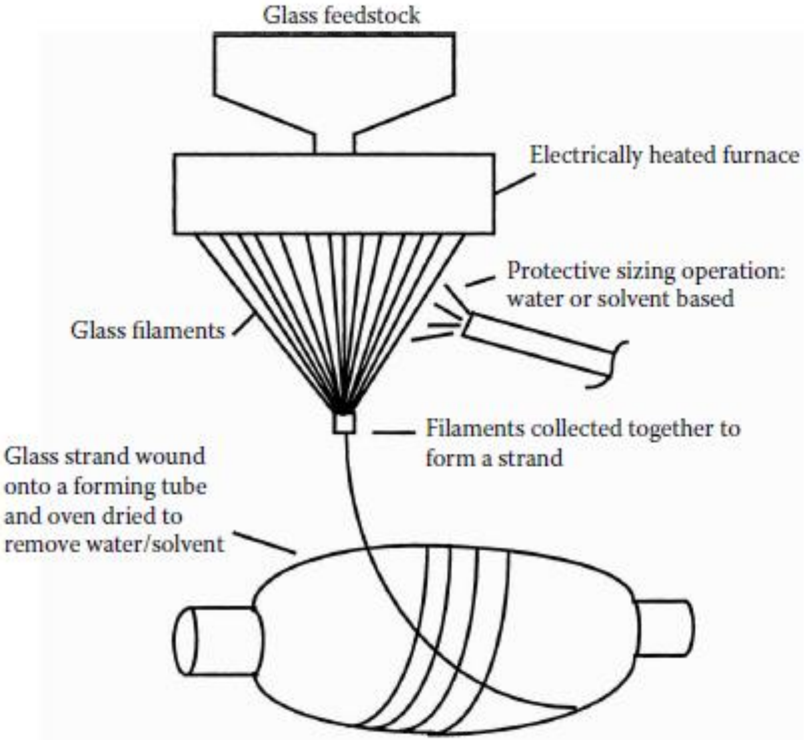

Figure 2.7: Schematic of manufacturing glass fiber form. Adapted from [25].

Over 95% of the fibers used in reinforced plastics are glass fibers, due to cheapness of production, easy to manufacture and possess high strength and stiffness with respect to the plastics with which they are reinforced.

Their low density, resistance to chemicals, insulation capacity are other bonus characteristics, although the one major disadvantage in glass is that it is prone to break when subjected to high tensile stress for a long time. The second one maybe we can say density of glass (used in aircraft structural parts) is nearly same as aluminum (used in aircraft structural parts).

However, it remains break-resistant at higher stress-levels in shorter time frames. This property mitigates the effective strength of glass especially when glass is expected to sustain loads for many months or years continuously.

Period of loading, temperature, moisture and other factors also dictate the tolerance levels of glass fibers and the disadvantage is further compounded by the fact that the brittleness of glass does not make room for prior warning before the catamorphic failure. But all this can be easily overlooked in view of the fact that the wide range of glass fiber variety lends themselves to fabrication processes like matched die-moulding, filament winding lay-up and so on. Glass fibers are available in the form of mates, tapes, cloth, continuous and chopped filaments, roving and yarns.

Addition of chemicals to silica sand while making glass yields different types of glasses.

2.4 Aramid Fibre (Kevlar®)

Aramid fibers, generally known as Kevlar, (Fig. 2.8) are made aromatic polyamides which are long polymeric chains and aromatic rings. They are structures in which six carbon s\atoms are bonded to each other and to combinations of hydrogen atoms. In aramid fibers, these rings occur and reoccur to form the fibers. They were initially used to reinforce automobile tires. Since then, they have also found other uses like bullet proof vests. As high strength applications, their use in power boats is not uncommon.

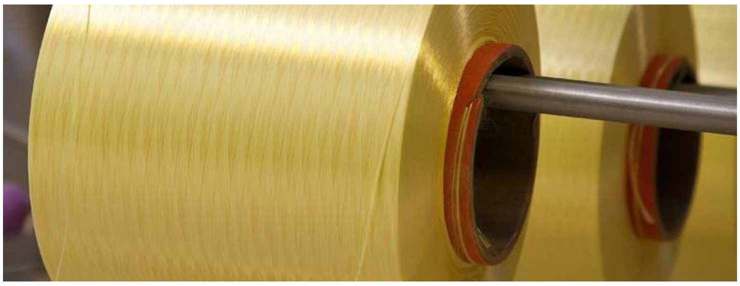

Figure 2.8: Aramid fiber. Taken from [37].

Aramid fibers held the distinction of having the highest strength-to-weight ratio of any commercially available reinforcement fiber at the time of their first commercial introduction in the early 1970s [38]. The earliest aramid fibers, under the trade name of Kevlar produced by E.I. Du Pont de Nemours, were initially targeted at reinforcement of tires and plastics. The characteristics of light weight, high strength, and high toughness have led to the development of applications in composites, especially in aerospace application.

An aramid fiber is an aromatic organic compound made of carbon, hydrogen, oxygen, and nitrogen (Fig. 2.9). Its advantages are low density, high tensile strength, low cost, and high impact resistance. Its disadvantages include low compressive properties and degradation in sunlight [25].

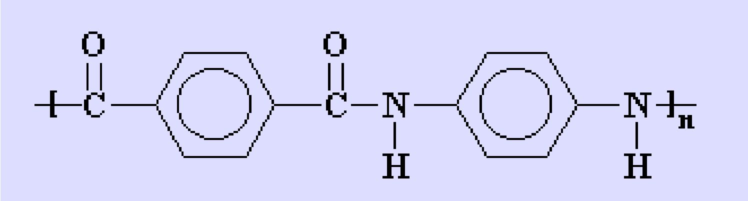

Figure 2.9: Aromatic compound of aramid fiber. Taken from [39].

Aramids have high tensile strength, high modulus and low weight. Impact-resistant structures can be produced from aramids. The density of aramid fibers is less than that of glass and graphite fibers. They are fire resistant apart from being high-temperature resistant and unaffected by organic solvents fuels. But their resistance in acid and alkaline media is poor. They are supple and allow themselves to be woven into matrices by simple processes. Aramid fibers have a negative coefficient of thermal expansion in the fiber direction and failure of aramid fibers is unique. When they fail, the fibers break into small fibers, which are like fibers within the fibers. This unique failure mechanism is responsible for high strength.

2.5 Carbon Fibre

Carbon fibers (Fig. 2.10) are very common in high-modulus and high-strength applications such as aircraft components [25]. The advantages of carbon fibers include high specific strength and modulus, low coefficient of thermal expansion, and high fatigue strength. The disadvantages include high cost, low impact resistance, and high electrical conductivity.

Carbon fiber products offer advantages for advanced material solutions such as light-weight, high-tensile strength, manufacturing flexibility and heat resistance [40].

Figure 2.10: Graphite fiber. Taken from [41].

Carbon fibers are now on the brink of broad commercialization after a 40 year period of development and use in specialized applications [42]. Their usage is growing rapidly, fueled by significant price reductions during the 1990s and increasing availability of raw material. Pozitive attitute in the performance/price ratio have resulted in the increased usage of composites in applications formerly held by metals and has enabled their use in other applications previously not possible with existing materials. Additionally, usage conditions provide increasingly favor designs for commercial products that are stronger, faster, lighter, and more fuel efficient. Not only for aerospace application, carbon fiber composites are now being adopted in fields such as automotive, civil industry, offshore oil and paper production application.

Carbon fibers are generally manufactured from three different types of raw materials: rayon, polyacrylonitrile (PAN) and pitch [25]. PAN is the most popular raw material to produce carbon fibers. The processes to manufacture carbon fibers from PAN and Pitch (petroleum pitch) are given in Figure 2.11. PAN fibers are first stretched five to ten times their length to improve their mechanical properties while pitch is melted and then passed through three heating processes. In the first process, called stabilization, the fiber is passed through a furnace between 200 and 300°C to stabilize its dimensions during the subsequent high-temperature processes. In the second process, called carbonization, it is pyrolized, is defined as the decomposition of a complex organic substance to one of a simpler structure by means of heat, in an inert atmosphere of nitrogen or argon between 1000 and 1500°C. In the last process, called graphitization, it is heat treated above 2500°C. The graphitization yields a microstructure that is more graphitic than that produced by carbonization. The fibers may also be subjected to tension in the last two heating processes to develop fibers with a higher degree of orientation.

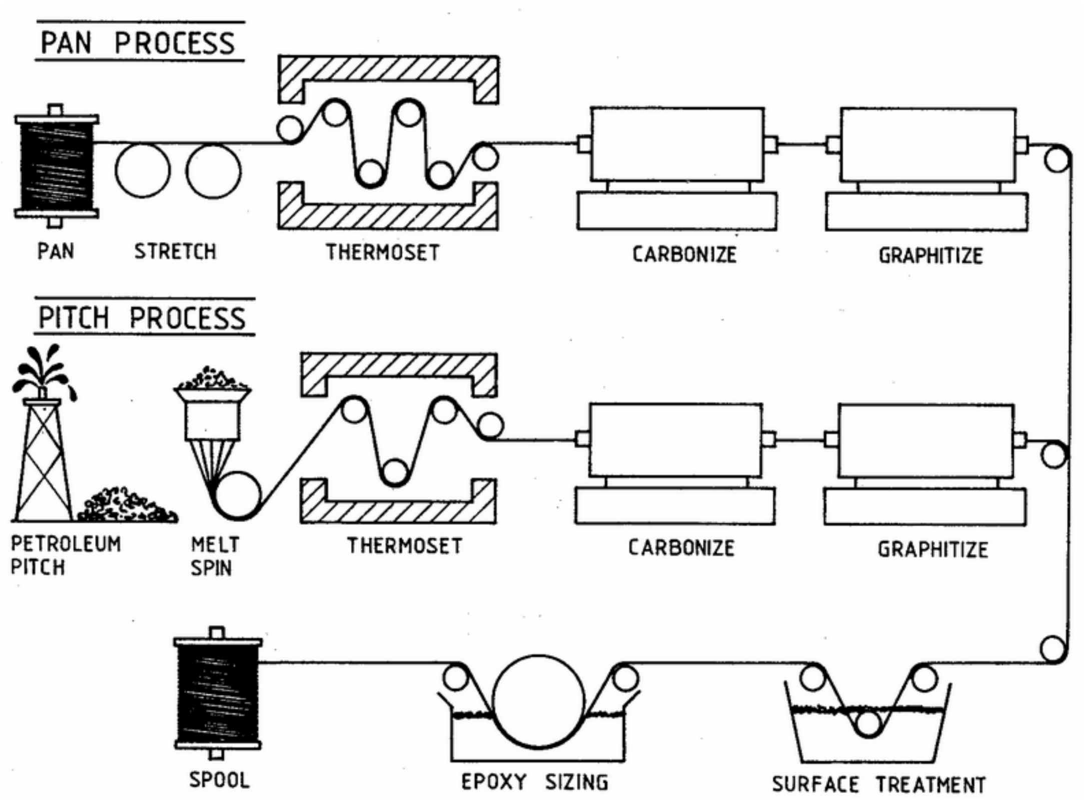

Figure 2.11: Manufacturing of graphite fibers. Taken from [43].

While use of the term carbon for graphite is permissible, there is one basic difference between the each of them. Element analysis of poly-acrylo-nitrile (PAN) based carbon fibers show that they consist of 91 to 94% carbon. But graphite fibers are over 99% carbon. The difference arises from the fact that the fibers are made at different temperatures. PAN-based carbon cloth or fiber is produced at about 1300ºC, while graphite fibers and cloth are graphitized at 2000 to 3000ºC.

The properties of graphite remain unchanged even at high temperatures, but its willingness to react eaisly with most metals at the fabrication stage or during use at very high temperatures is often a stumbling block, as seen in aluminum matrices when carbides are produced at the interface.

Graphite fibers are some of the stiffer fibers known generally. The stiffness of the fiber is as high as the graphite content. But a major drawback is that stiffness and strength are inversely proportional to each other.

Forbidding costs make the use of graphite fibers prohibitive. The best glass fibers are far less expensive than the cheapest, lowest quality of graphite, and in PAN-base fibers, other raw materials too are equally expensive. The carbonization and graphitization are time-consuming, apart from demanding excessive energy, materials and close controls throughout the process.

Cheaper pitch base fibers are now being developed, with greater mechanical performance and there are many possibilities of the increased usage of graphite fibers.

CHAPTER THREE

EXPERIMENTAL DATA

For this thesis study, we use carbon-epoxy composite materials ABS5139C1219A (AIMS 05-01-001) [44].

For adhesive we have chosen Hysol® EA 9394 [45], very common used adhesive as structural application in aerospace and aircraft components.

3.1 Tool Preparation

While performing test, getting real results or almost real results is so important. For this reason preparing tool or using applicable tool is too important to prepare the correct test specimens. Before performing tests, we prepared two different types of tools. We named them tool 1 and tool 2.

3.1.1 Tool 1

Tool 1 is for preparing composite materials, to lay up carbon fiber-epoxy prepreg. It has a flat surface, so that the surface of the composite part must be smooth. The geometric dimensions are given in figure 3.1.

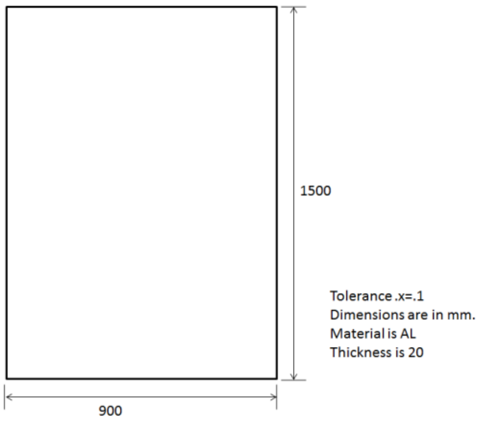

Figure 3.1: Technical drawing of tool 1.

3.1.2 Tool 2

Tool 2 is for bonding of test samples. It helps us to bring the parts together, in line and to control the adhesive thickness that we apply to bond the parts. It composes of two parts. Part 1 is to align the samples (Fig. 3.2); part 2 is to press the samples (Fig. 3.3). Figure 3.2 gives the technical drawing of tool 2.

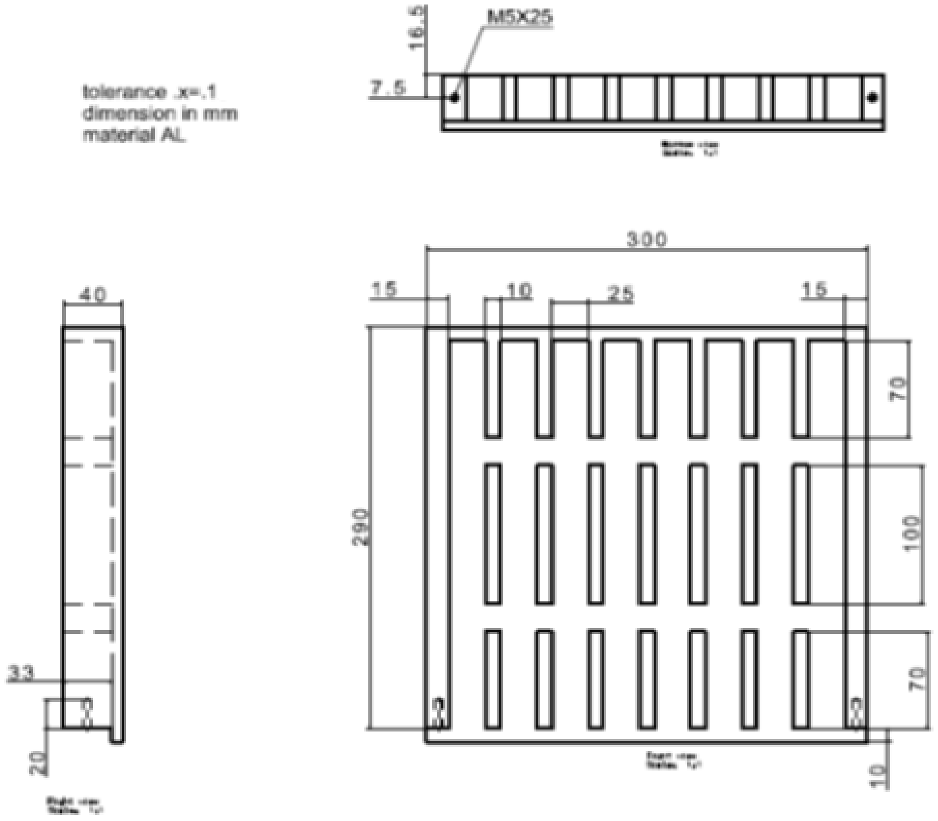

Figure 3.2: Technical drawing of part 1 of tool 2.

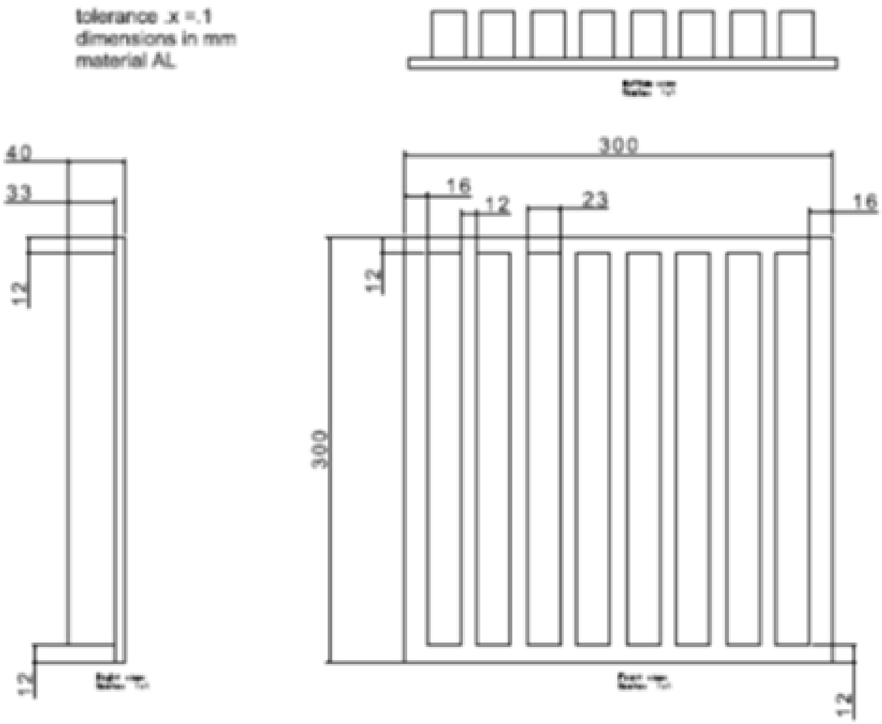

Figure 3.3: Technical drawing of part 2 of tool 2.

3.2 Test Specimens

Using tool 1, we lay up the carbon-epoxy prepreg material. Before this operation we prepared ply orientation table for each sample (0^0, 15^0, 30^0, 45^0, 60^0, 75^0, 90^0). Fibre orientations are shown in the design $[(0)_{12}]$, $[(+15/-15)_3(-15/+15)_3]$, $[(+30/-30)_3(-30/+30)_3]$, $[(+45/-45)_3(-45/+45)_3]$, $[(+60/-60)_3(-60/+60)_3]$, $[(+75/-75)_3(-75/+75)_3]$ and $[(+90/-90)_3(-90/+90)_3]$. Below we can find the orientation of direction for each sample. In appendix A, Tables A.1 through Table A.7 give the ply directions.

We have prepared the tool 1 for laying-up just applying release agent (Frekote 700). We apply release agent at least three coats by allowing 15 minutes of drying time in between and cross angle. First we apply through the 0^0 direction, then 90^0 and last one again through the 0^0 direction. Prior to lay up we cure the release agent at room temperature for 60 minutes. In this time period, in the clean room (controlled contamination area) we cut the prepreg and prepare the set of samples. Temperature of clean room is 21^0C and humidity of area is %45. We lay up the prepreg as applicable to the given direction. After laying up every first layer we apply compaction for 15 minutes. This compaction helps us to remove the gas or air between plies. We apply same compaction fifth and ninth layers. At the end final vacuum is applied.

And then we prepare the lay-up for autoclave cure. To control the temperature and pressure we place two thermocouples and two vacuum pumps on the tool. Thermocouple places are chosen according to temperature rises up, one for higher (leading) one for lower (lagging) determined before. Tool is ready for cure operation.

Curing operation must be held in autoclave with the given values below:

a) Cure temperature (^{0}C): 180 ±5

b) Pressure (bar): 6.5 ± .30

c) Hold time (min): 120-190

d) Heat up rate (^{0}C/min): 0.5-3.5

e) Cold down rate (^{0}C/min): 0.5-3.5

After curing operation is completed autoclave gives us an autoclave report, which includes the information of curing (Table 3.8). For example, when the autoclave is closed the air temperature of autoclave is 36^{0}C while thermocouple number 36 is 30.3^{0}C; thermocouple number 37 is 29.7^{0}C. The pressure is 0. For example, 15 minutes later air temperature is 42.1^{0}C while PTC36 is 37.2^{0}C; PTC37 is 36.5^{0}C. The pressure is 4.3 bars.

After seventy minutes passed, air thermocouple is 126.5^{0}C, PTC36 is 107.6^{0}C and PTC37 is 106.1^{0}C. The difference between air thermocouple and PTC37 is more than 20^{0}C. In this case, the autoclave is taken in to standby mode automatically. It means the autoclave waits the lagging thermocouple reaches the leading thermocouple.

After 401.8 minutes later, autoclave starts to cool down. It means the curing operation is completed. After this moment pressure on the part is off. One of the thermocouple reaches 40^{0}C the door of the autoclave is open.

Table 3.1: Autoclave report.

Time	Mins	AIRTC Deg. ^{0}C	PRESS Bar	PTC36 Deg. ^{0}C	PTC37 Deg. ^{0}C	MON33
00:07:21	0	36.0	0.0	30.3	29.7	-635.3
00:07:22	0	36.0	0.0	30.3	29.7	-635.3
00:08:22	1	35.3	0.1	31.0	30.0	-637.6
00:09:22	2	37.8	0.4	31.7	30.4	-635.3
00:12:22	5	39.7	1.3	33.0	31.6	-630.6
00:13:22	6	40.0	1.6	33.5	32.0	-629.4
00:17:22	10	40.9	2.8	34.7	33.9	-636.5
00:18:22	11	41.2	3.1	35.2	34.4	-635.3
00:19:22	12	41.4	3.4	35.7	34.9	-634.1
00:20:22	13	41.6	3.7	36.2	35.4	-635.3
00:22:23	15	42.1	4.3	37.2	36.5	-634.1
00:50:22	43	72.5	6.6	58.2	57.8	-623.5
00:51:23	44	74.2	6.6	59.8	59.2	-624.7
01:00:23	53	87.1	6.6	73.5	72.7	-625.8
01:07:23	60	106.7	6.5	85.8	84.7	-624.7
01:08:23	61	109.2	6.5	87.9	86.7	-622.3
01:16:23	69	126.0	6.5	105.6	104.1	-616.4
01:22:22	75	127.4	6.5	115.6	114.2	-609.3
01:23:22	76	127.4	6.5	116.8	115.3	-609.3
01:37:22	90	127.1	6.5	124.9	124.0	-603.4
01:47:23	100	127.5	6.5	126.4	125.8	-602.2
03:27:22	200	137.7	6.5	137.8	137.5	-582.2
04:17:22	250	193.8	6.5	176.1	173.9	-455.8
04:18:22	251	191.4	6.4	177.6	175.5	-448.7
04:19:22	252	189.6	6.4	178.6	176.8	-444.0
04:20:22	253	190.4	6.4	179.9	178.1	-438.1
04:28:22	261	183.6	6.4	183.0	182.2	-421.6
04:37:22	270	183.5	6.5	183.8	183.1	-416.8
06:47:22	400	180.2	6.5	179.8	179.3	-418.0
06:48:22	401	180.1	6.5	179.8	179.3	-418.0
06:49:12	401.8	180.1	6.5	179.8	179.3	-416.8
06:49:23	402	180.1	6.5	179.7	179.3	-338.9
06:50:24	403.1	177.0	6.4	179.3	179.0	46.1
08:30:02	502.7	45.5	6.5	48.6	48.5	37.8
08:37:49	510.5	24.2	0.2	40.9	41.5	30.7

In the autoclave report, there are two thermocouples, one is leading and one is lagging, when the lagging thermocouple reaches the minimum cure temperature the cure cycle is starting. After 251 minutes later the lagging thermocouple reached the minimum curing temperature. All information of this curing operation is shown in the Figure 3.4 below.

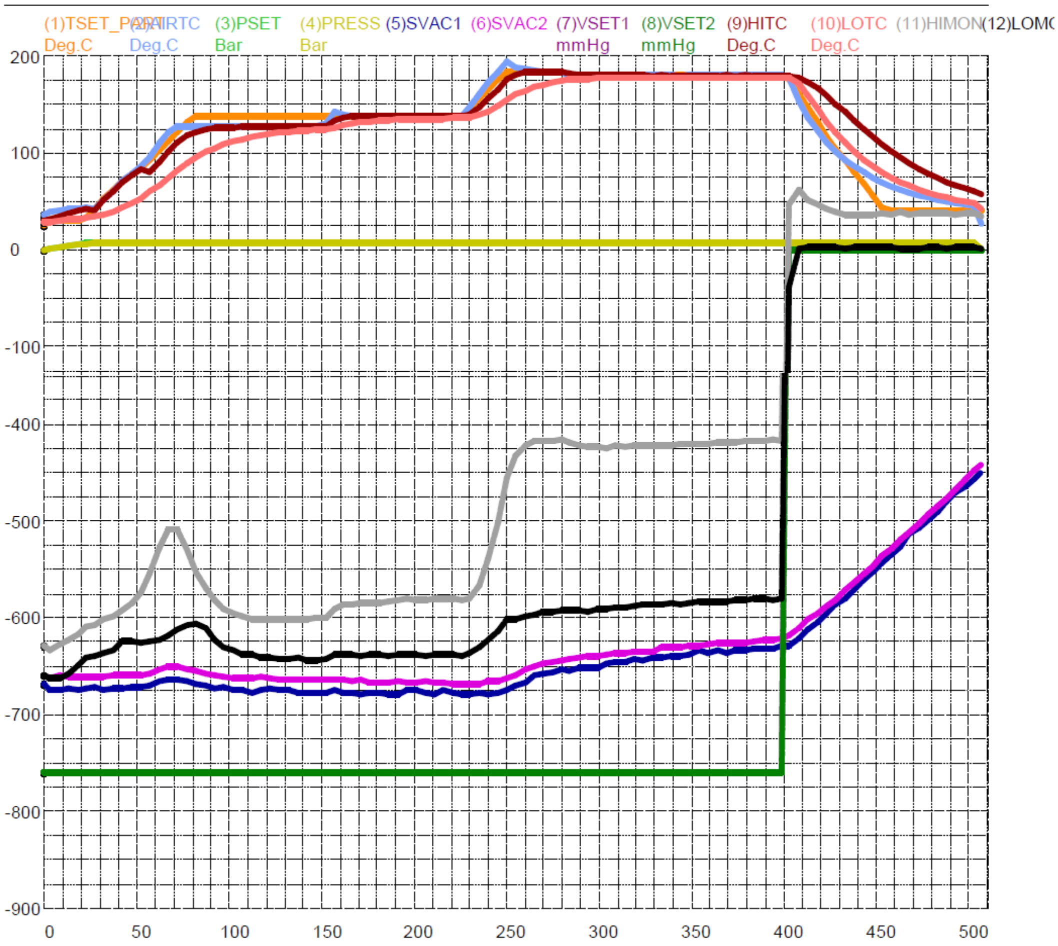

Figure 3.4: Curing information.

The parts are shown in the Figure 3.5 after curing. Direction of fiber is written by hand to distinguish them. After parts cured, we cut the part in to pieces that we use for bending and bonding test.

Figure 3.5: Parts after curing.

3.2.1 Bending Test Specimen

We have prepared the bend test (three point bend test) specimen according to ASTM D792 [46]. In the Figure 3.6 below shows the part that we used for bend test 0 degree sample number three.

Figure 3.6: 0 degree test sample for bending.

3.2.2 Bonding Test Specimen

We have prepared the tensile test specimen according to ASTM D3039 [47]. In the Figure 3.7 below shows the part that we used to bond and then tensile test of bonding.

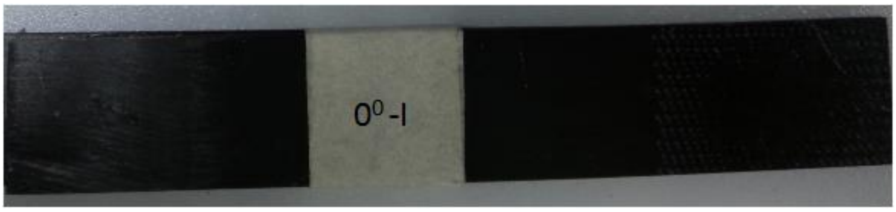

Figure 3.7: 0 degree test sample for bonding.

3.3 Bonding Operation

To bond the samples for bonding test we have chosen Hysol EA 9394 [46]. It is a two-part adhesive (commonly used for aircraft), which can be cured at room temperature and gives us excellent strength to 177^0C/350^0F. It can be also stored in room temperature. Since it is a two-part adhesive we call them part A and part B. Color of part A is gray, B is black and mixture of them is also gray. Mix ratio depends on by weight and the ratio is 100 g from part A and 17 g from part B. Pot life of mixture is 90 minutes up to a mixture of 450 g.

3.3.1 Preparation of Bonding Surface

Caution: It is strongly recommended to use of personal protective equipments (PPE) given in Figure 3.8 such as gloves, mask and vacuum cleaner.

Figure 3.8: Personal protective equipments.

Before bond the parts we clean the bond surface with the cleaner which is applicable to carbon composite materials. Cleaning of adherent materials and methods are given in the table 3.9 [48].

Table 3.2: Material type and cleaning method.

Thermosets			
Adherent material	Cleaning	Abrasion or chemical treatment	Method
Epoxy, Epoxide resins	Degrease with acetone or MEK	Abrade using medium-grit emery paper	Repeat degreasing step

With the abrasive paper (Fig. 3.9), grain size 180 or finer, we have sanded the surface smoothly; just sanding the resin, no touching the fibers. We can easily realize that either we sand resin or fiber just observing the dust which is produced by sanding. If the color of dust is grey it means resin is sanded, if the color of dust is getting darker it means fiber is sanding. The aim of this sanding operation is to increase the surface contact area of adhesive. We wipe out the surface with a solvent soaked lint free cloth. And then wipe out the surface immediately with a lint free dry cloth. We do not allow the solvent dry out on the surface. We repeat this cleaning operation up to no residue observed on the cleaning cloth. Quality of bonding depends on some reasons. One of them is cleaning. For this reason cleaning of contact area is so important. The purpose of this cleaning operation is to increase the quality of contact surface area.

Figure 3.9: Abrasive paper. Taken from [49].

3.3.2 Application and Curing of Adhesive

We apply the mixture of adhesive both surfaces of samples area of 25x25mm^2 shown in figure 3.10.

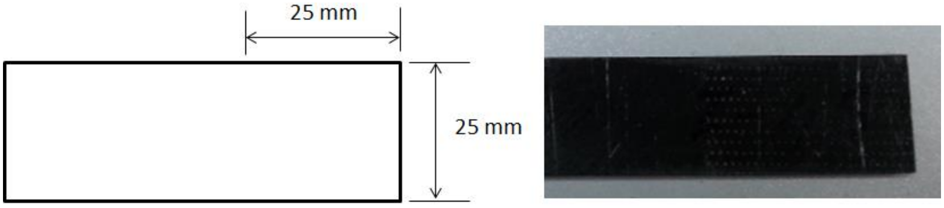

Figure 3.10: Bond area.

To adjust the bond thickness we used small metal parts (Fig. 3.11), apart from bond area, whose thickness is 2,5 mm. It means that adhesive thickness is nearly 0,2 mm (Sample thickness is 2,3 mm; metal part thickness is 2,5 mm). Figure 3.12 shows that the alignment of metal parts in the bonding operation on the tool.

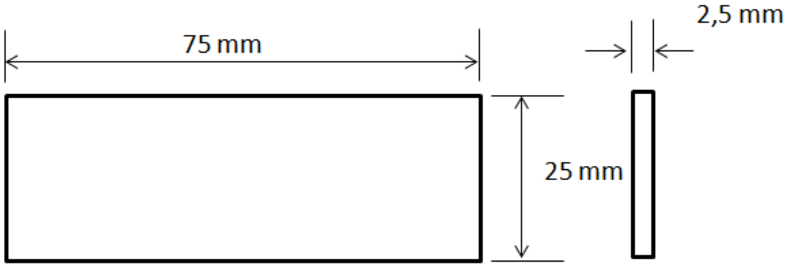

Figure 3.11: Metal parts used for adjusting the thickness of adhesive.

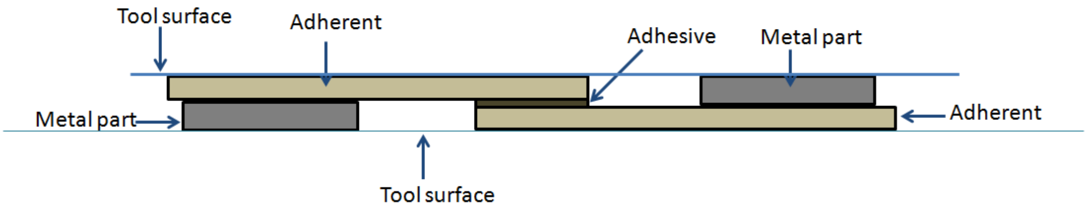

Figure 3.12: Alignment of metal parts.

The adhesive (Hysol EA9394) may be cured for 3 to 5 days at 25^0C/77^0F to achieve normal performance [45]. Accelerated cures can be applied up to 93^0C/200^0F as an alternative. For example, 1 hour 66^0C/150^0F will give complete cure. We cured our bonding samples at 66^0C in the oven for just 1 hour.

3.4 Test Operations

After preparing all of samples, we perform experiments. Experiments (both bending and bonding test) were done with the machine Tenson WDW-T50.

3.5 The Three Point Bend Test Theory

The three point bending flexural test provides modulus of elasticity in bending. Flexure test require the load to be applied to the midsection of the sample so that it is bent into a “U” or “V” shape with the outside surface experiencing tensile forces (Fig. 3.13) and inside face experiencing compressive forces [50]. An example of set-up is shown in the Figure 3.14.

When the cross-section of used sample is rectangular the test is called as rectangular three point bending test (Fig. 3.15).

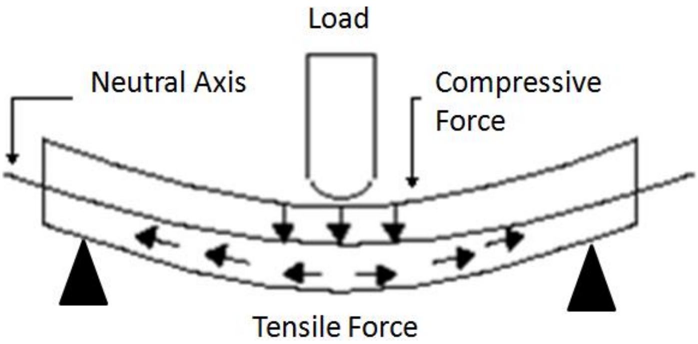

Figure 3.13: Tensile and compressive forces. Adapted from [50].

Figure 3.14: The three point bending test set-up. Taken from [50].

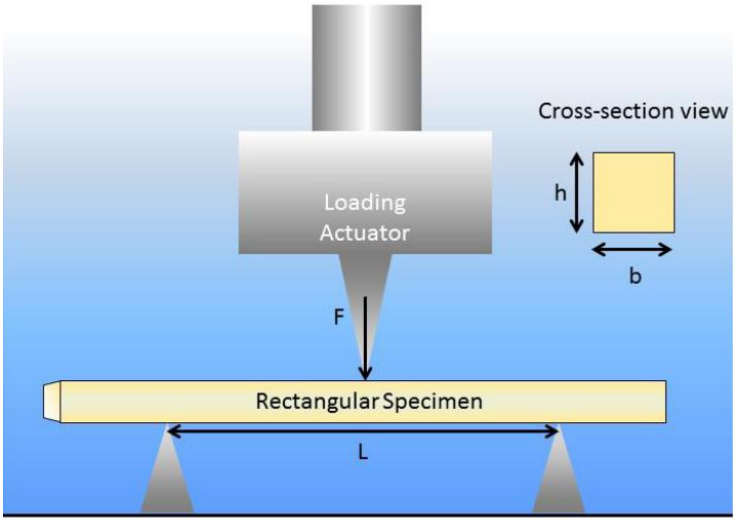

Figure 3.15: Rectangular three point bending test. Adapted from [51].

For example, a rectangular test specimen is subjected to a three point bending test. The specimen is 100 mm long, 25 mm wide (b) and 2,3 mm height (h). The specimen placed on two supports which are 80 mm apart (L) from each other, and the actuator is applying a force in the exact middle of the support (L/2). Just before failure, Tenson WDW-T50 records a force (F) of 2,2 kN, and a deformation (**δ**) of 8 mm. Now, we need to determine the maximum flexural strength (**σ**) and Young's Modulus (**E**) of the test specimen. To do this task we are going to use the two following equations:

$$\sigma = \frac{My}{I}$$ **Eq. 3.1** [52]

$$\delta = \frac{FL^3}{48EI}$$ **Eq. 3.2**

Where M is the moment applied at the middle of the specimen, δ is displacement y is the distance from the center of the specimen to the convex surface and *I* is the "polar moment of inertia", a term used to define how the geometry of the specimen influences its reaction to loads.

Firstly, we should calculate the reaction forces at the support. In this case we have two unknown values. Therefore we should use two equations to solve the system. According to static mechanics we may use following two equations:

$$\sum F_y = 0$$ **Eq. 3.3**

$$\sum M = 0$$ **Eq. 3.4**

From these equations using Eq.3.3,

$$\sum F_y = -F + F_{left\ support} + F_{right\ support} = 0$$

$\sum F_y = -2200 + F_{left\ support} + F_{right\ support} = 0$ or $F_{left\ support} + F_{right\ support} = 2200$ N **Eq. 3.5**

Now using Eq.3.4,

$$\sum M_{left\ support} = (-F * L/2) + (F_{right\ support} * L) = 0$$

$$(-2200 * 0{,}08/2) + (F_{right\ support} * 0{,}08) = 0$$

Solving this equation for $F_{right\ support}$ we find that:

$$F_{right\ support} = 1100 \text{ N}$$

Now, substituting this

$F_{right\ support}$ = 1100N value in the Eq.3.5; we find $F_{left\ support}$ = 1100 N

This means we have solved reaction forces problem at the support. We can calculate the moment acting at the midpoint of the specimen by looking at half of the specimen and using the following equation:

$$Moment = \sum Force * distance \qquad \textbf{Eq. 3.6}$$

….in our case….

$$M = F_{right\ support} * L/2$$

$$M = 1100 * 0{,}04 = 44 \text{ Nm}$$

Next we can calculate y, the distance from the center of the specimen to the convex surface:

$$y = h/2 \qquad \textbf{Eq. 3.7}$$

…from our values…

$$y = 0{,}0023 / 2 = 0{,}00115 \text{ m}$$

Next we can calculate I, the polar moment of inertia. For rectangular cross-section, the equation is:

$$I_{rectangle} = (bh^3) / 12 \qquad \textbf{Eq. 3.8}$$

…from our values…

$$I_{rectangle} = [0{,}025 * (0{,}0023)^3] / 12 = 2{,}53e^{-11} \text{ m}^4$$

Up to here we calculate M, y and I. We are ready to calculate the maximum flexural stress of the specimen, by using Eq.3.1:

$$\sigma = \frac{My}{I} = \frac{44 * 0{,}00115}{2{,}53e-11} = 2e^9 = 2\text{GPa}$$

Finally, we can calculate Young's modulus, by using Eq.3.2:

$$\delta = \frac{FL^3}{48EI} \text{ …rearranging this eq. for } E = \frac{FL^3}{48\delta I}$$

$$E = [2200 * (0{,}08)^3] / [48 * (0{,}008) * 2{,}53e^{-11}]$$

$$E = 1{,}16e^{11} = 116 \text{ GPa}$$

With the given equations and defined in example, we calculate the Young's Modulus of our samples separately.

3.6 Tensile Lap Shear Strength (Bond Strength Performance) Test Theory of Bonding

Bonded material is pulled from their ends to deform the bonded area as seen in the Figure 3.16.

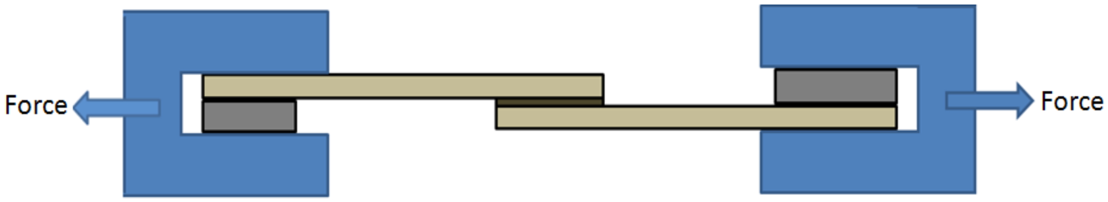

Figure 3.16: Apparatus of shear test of bonded material.

Shear stress can be defined as the load acting parallel to the face in question per unit of effected are as shown in following equation [53].

$$\tau = \frac{F}{A}$$ **Eq. 3.9**

Where F is the load acting parallel to the element face, A is the cross-sectional area measured in m^2.

CHAPTER FOUR

RESULTS

Firstly, we performed the bending test (rectangular three point bending test). Then, tensile lap shear strength (bond strength performance) of bonding samples of carbon material is tested. Test environment conditions are:

a) Test lab in the university.
b) Temperature is 23^0C
c) Humidity is %45.
d) Velocity is 2mm /min

4.1 Rectangular Three Point Bending Test Results

Let’s examine deeply the results for each sample.

4.1.1 0 Degree Samples

For 0 degree we performed 5 experiments, it means 5 different samples are used for each test. We name them like bnd_0_I. It means first sample of bend test for 0 degree. And goes like this, bnd_0_II, bnd_0_III, bnd_0_IV and bnd_0_V. Detailed calculation of all different type of angles of samples are given in appendix B.

We have finished calculation of Young’s Modulus of 0 degree samples. In the table 4.1 below, we can find all of the results of 0 degree samples. Figure 4.1 gives the graphical distribution of results.

Table 4.1: Young's Modulus of 0 degree samples.

0 degree sample numbers	E (GPa)
bnd_0_I	123,5
bnd_0_II	125,4
bnd_0_III	125,32
bnd_0_IV	124,2
bnd_0_V	122,81
bnd_0	124,25 ±1,24

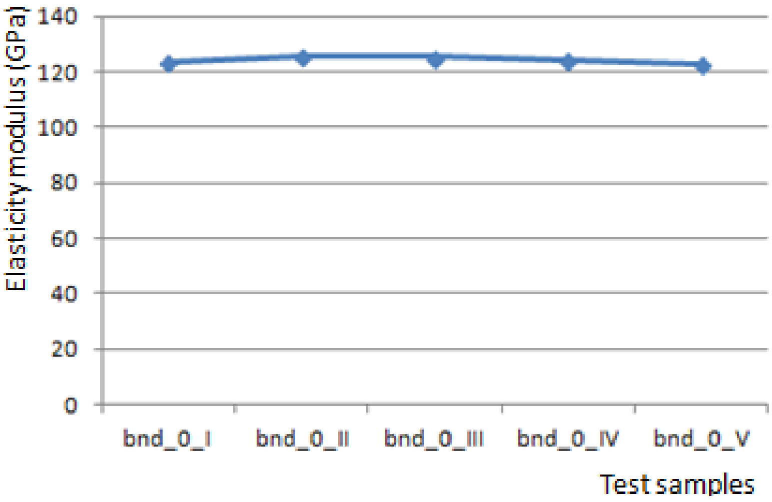

Figure 4.1: Graphical representation of bnd_0 results.

4.1.2 15 Degree Samples

Secondly, we calculate Young's Modulus of 15 degree samples. Similarly, we have five samples and we name these samples like 0 degree samples, bnd_15_I. it means sample number 1 of 15 degree samples. And goes like same way, bnd_15_II, bnd_15_III, bnd_15_IV and bnd_15_V.

Using same procedure and steps for bnd_0, we calculate Young's Modulus of 15 degree samples.

We have finished the calculation of Young's Modulus of 15 degree samples. In the Table 4.2 below we can find all of the results of 15 degree samples. Figure 4.2 gives the graphical representation of results.

Table 4.2: Young's Modulus of 15 degree samples.

15 degree sample numbers	E (GPa)
bnd_15_I	101,44
bnd_15_II	105,75
bnd_15_III	104,44
bnd_15_IV	101,77
bnd_15_V	102,90
bnd_15	103,26 ± 1,82

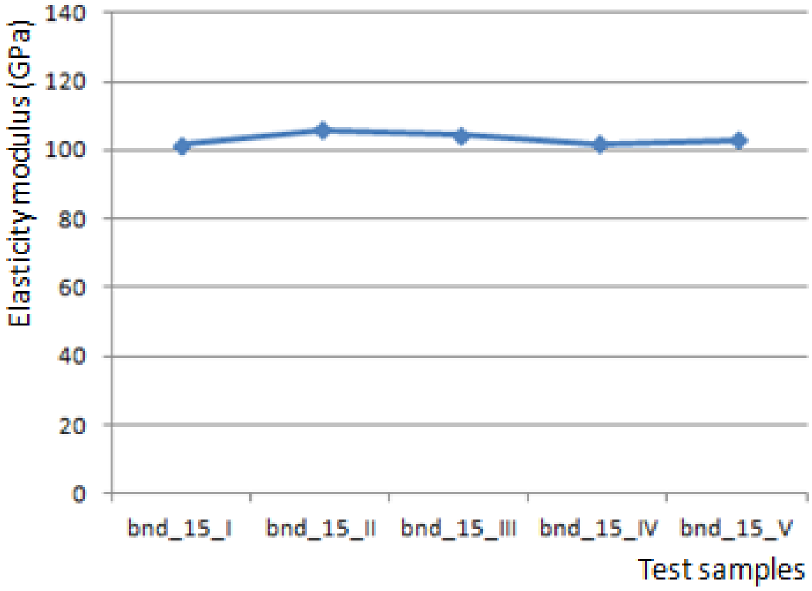

Figure 4.2: Graphical representation of bnd_15 results.

4.1.3 30 Degree Samples

Thirdly, we calculate Young's Modulus of 30 degree bending test samples. Similarly, we have five samples and we name these samples like 0 degree samples, bnd_30_I. It means sample number 1 of 30 degree samples. And goes like same way, bnd_30_II, bnd_30_III, bnd_30_IV and bnd_30_V.

Using same procedure and steps for bnd_0, we calculate Young's Modulus of 30 degree bending test samples.

We have finished the calculation of Young's Modulus of 30 degree samples. In the table 4.3 below, we can find all of the results of 30 degree samples. Figure 4.3 gives the graphical representation of results.

Table 4.3: Young’s Modulus of 30 degree samples.

30 degree sample numbers	E (GPa)
bnd_30_I	59,14
bnd_30_II	57,0
bnd_30_III	58,91
bnd_30_IV	57,00
bnd_30_V	56,99
bnd_30	57,81 ±1,11

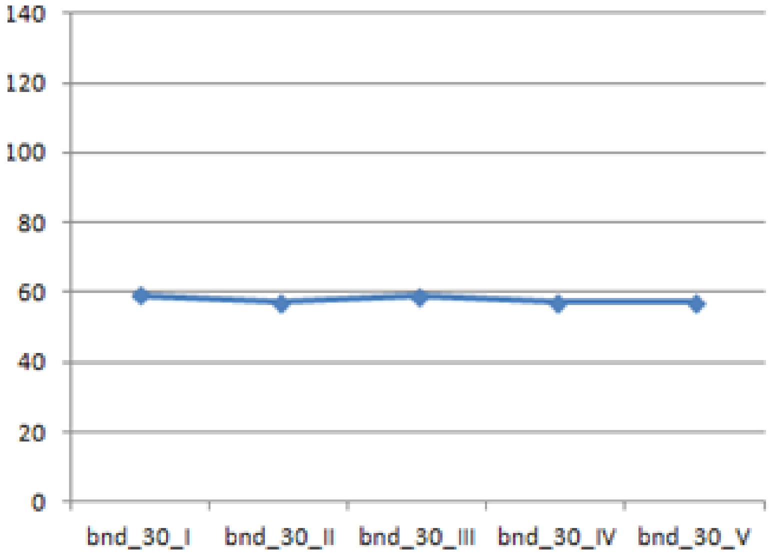

Figure 4.3: Graphical representation of bnd_30 results.

4.1.4 45 Degree Samples

Fourthly, we calculate Young’s Modulus of 45 degree bending test samples. Similarly, we have five samples and we name these samples like 0 degree samples, bnd_45_I. It means sample number 1 of 45 degree samples. And goes like same way, bnd_45_II, bnd_45_III, bnd_45_IV and bnd_45_V.

Using same procedure and steps for bnd_0, we calculate Young’s Modulus of 45 degree bending test samples.

We have finished the calculation of Young’s Modulus of 45 degree samples. In the Table 4.4 below we can find all of the results of 45 degree samples. Figure 4.4 gives the graphical representation of results.

Table 4.4: Young's modulus of 45 degree samples.

45 degree sample numbers	E (GPa)
bnd_45_I	19,02
bnd_45_II	18,34
bnd_45_III	18,92
bnd_45_IV	18,95
bnd_45_V	18,33
bnd_45	18,71 ± 0,35

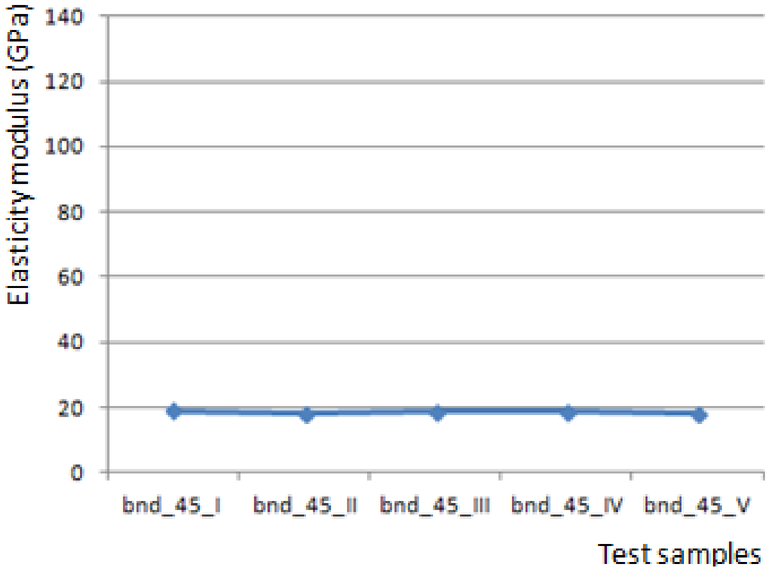

Figure 4.4: Graphical representation of bnd_45 results.

4.1.5 60 Degree Samples

Now, we calculate Young's Modulus of 60 degree bending test samples. Similarly, we have five samples and we name these samples like 0 degree samples, bnd_60_I. It means sample number 1 of 60 degree samples. And goes like same way, bnd_60_II, bnd_60_III, bnd_60_IV and bnd_60_V.

Using same procedure and steps for bnd_0, we can calculate Young's Modulus of 60 degree bending test samples.

We have finished the calculation of Young's Modulus of 60 degree samples. In the table 4.5 below, we can find all of the results of 60 degree samples. Figure 4.5 gives the graphical representation of results.

Table 4.5: Young's Modulus of 60 degree samples.

60 degree sample numbers	E (GPa)
bnd_60_I	12,38
bnd_60_II	12,53
bnd_60_III	11,99
bnd_60_IV	12,28
bnd_60_V	12,22
bnd_60	12,28 ±0,2

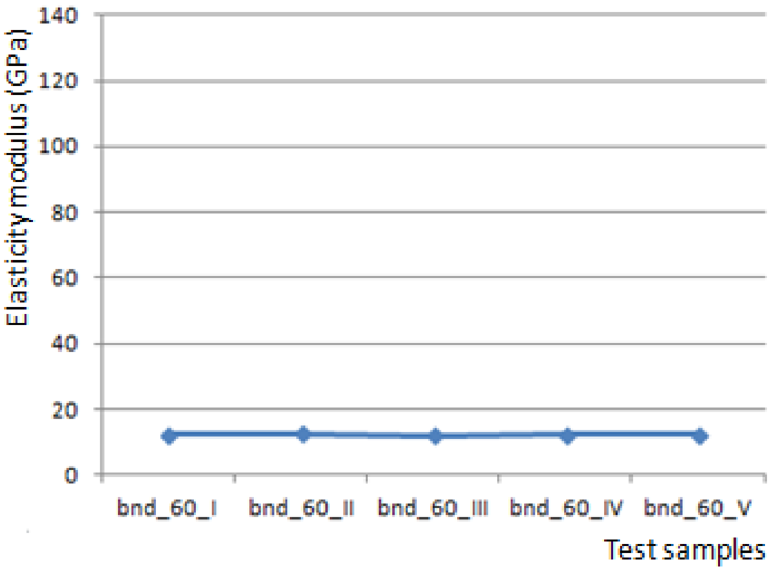

Figure 4.5: Graphical representation of bnd_60 results.

4.1.6 75 Degree Samples

Last one, we calculate Young's Modulus of 75 degree bending test samples. Similarly, we have five samples and we name these samples like 0 degree samples, bnd_75_I. It means sample number 1 of 75 degree samples. And goes like same way, bnd_75_II, bnd_75_III, bnd_75_IV and bnd_75_V.

Using same procedure and steps for bnd_0, we can calculate Young's Modulus of 75 degree bending test samples.

We have finished the calculation of Young's Modulus of 75 degree samples. In the table 4.6 below, we can find all of the results of 75 degree samples. Figure 4.6 gives the graphical representation of results.

Table 4.6: Young's Modulus of 75 degree samples.

75 degree sample numbers	E (GPa)
bnd_75_I	10,01
bnd_75_II	9,42
bnd_75_III	8,70
bnd_75_IV	9,49
bnd_75_V	8,76
bnd_75	9,28 ±1,09

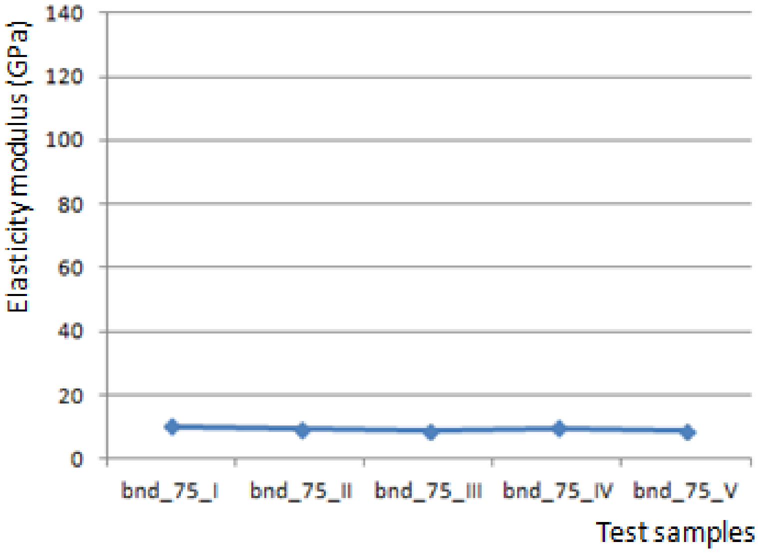

Figure 4.6: Graphical representation of bnd_75 results.

Graphic representation of load vs. displacement of bending test can be seen in the figure 4.7 below. In the graph, 0 degree samples have highest load minimum displacement, 15 degree samples have lower load higher displacement and goes like this. When the angle orientation departs from 0 degree, load decreases and displacement increases.

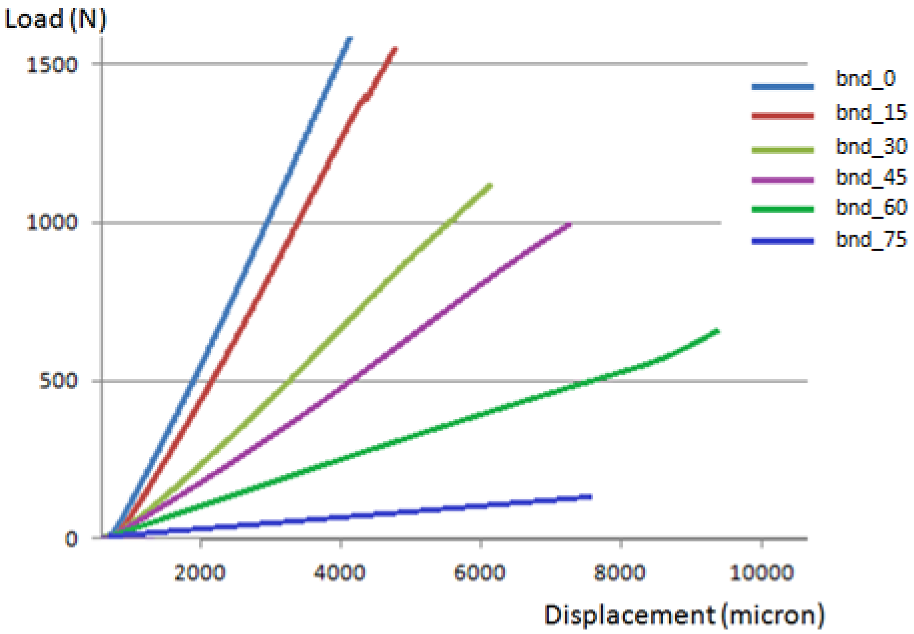

Figure 4.7: Graphic representation of load vs. displacement.

4.2 Tensile Lap Shear Strength of Single Lap Joint of Carbon

We have finished rectangular three point bending tests. After this, we can see the results of shear strength of single lap joint of carbon. In other words, we can detect the effect of ply angle on bonding strength. In this test we try to see the effect of angle orientation on bonding strength carbon as single lap joint. We call the results slj_c_*angle_sample* number.

4.2.1 Slj_c_0

To get consistent results we have performed five tests for each angle orientation. To differentiate them we named them shear tests of bonding samples of carbon as single lap joint (slj_c_0_I). It means test sample one of 0 degree angle of carbon. And goes like this, slj_c_0_II, it means sample one of 0 degree angle of carbon, slj_c_0_III, slj_c_0_IV and slj_c_0_V.

To calculate the shear strength we use the Eq.3.9.

We can see the test part of slj_c_0_I in the Figure 4.8.

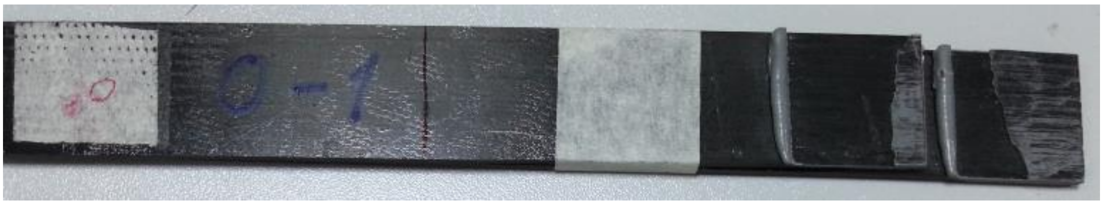

Figure 4.8: Test sample of slj_c_0_I.

We get result after experiment for this type of joint (slj_c_0_I) 11,16 kN. In this experiment our part get broken when the computer shows us the value 11,16 kN. Bonded area geometry is shown in the Figure 4.9. This area is same for all type of test samples. No deformation on part especially on the bonded surface is observed but adhesive is scattered around the lab.

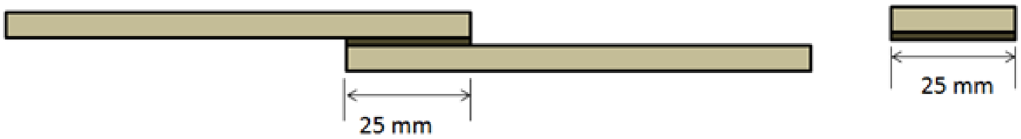

Figure 4.9: Bonded area of test sample.

Detailed calculations of tensile lap shear strength of single lap joints of carbon fibre are given in appendix C.

We have finished the calculation of tensile lap shear strength of 0 degree samples. In the table 4.7 and Figure 4.10 below, we can find all of the results of 0 degree samples and graphical representation of results.

Table 4.7: Tensile lap shear strength of 0 degree samples.

0 degree sample numbers	τ (MPa)
slj_c_0_I	17,86
slj_c_0_II	18,37
slj_c_0_III	19,14
slj_c_0_IV	18,8
slj_c_0_V	17,87
slj_c_0	18,41 ±0,57

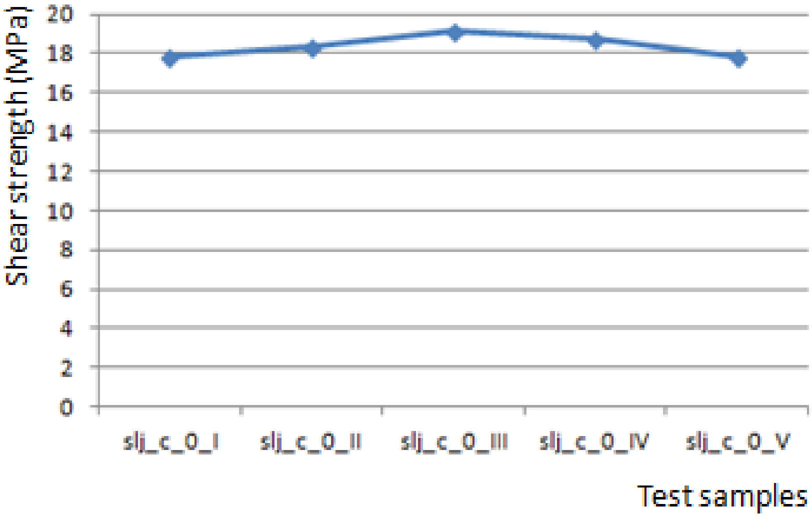

Figure 4.10: Graphical representation of slj_c_0 results.

4.2.2 Slj_c_15

Same as slj_c_0 we perform five experiments, and we named them like previous one. slj_c_15_I it means test sample one of 15 degree angle of carbon. And then goes like this way, slj_c_15_II, slj_c_15_III, slj_c_15_IV and slj_c_15_V. For the first experiment our result is 7,6 kN. Area is same. Sample I and II are shown in the Figure 4.11.

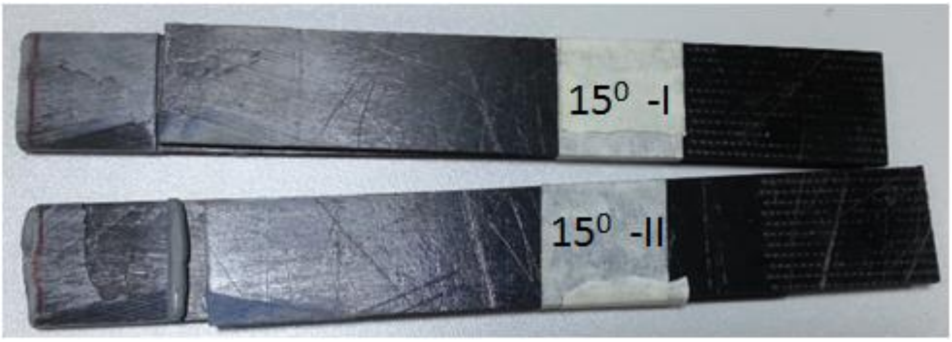

Figure 4.11: Test sample of slj_c_15_I and slj_c_15_II.

We observed in this experiment visually that one layer of prepreg is broken away from the test part as shown in Figure 4.12 in the bonded area. Adhesive is scattered around the lab and deformation on the bonded surface is observed.

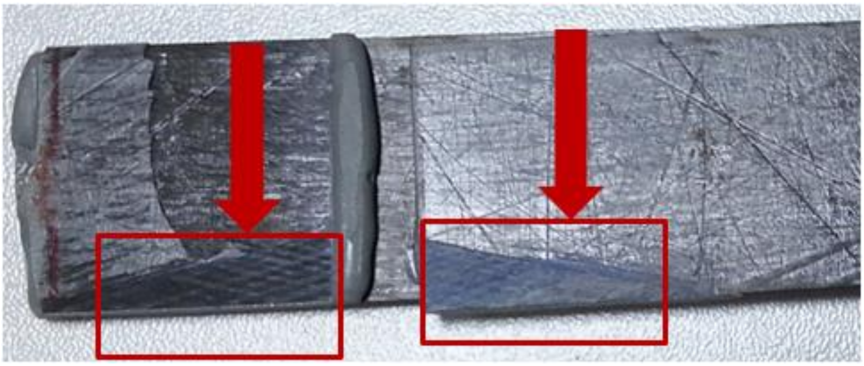

Figure 4.12: Bonded surface deformation after adhesive break.

We have finished the calculation of tensile lap shear strength of 15 degree samples. In the table 4.8 and Figure 4.13 below, we can find all of the results of 15 degree samples and graphical representation of results.

Table 4.8: Tensile lap shear strength of 15 degree samples.

15 degree sample numbers	τ (MPa)
slj_c_15_I	12,16
slj_c_15_II	12,64
slj_c_15_III	12,32
slj_c_15_IV	12,37
slj_c_15_V	12,96
slj_c_15	12,49 ±0,31

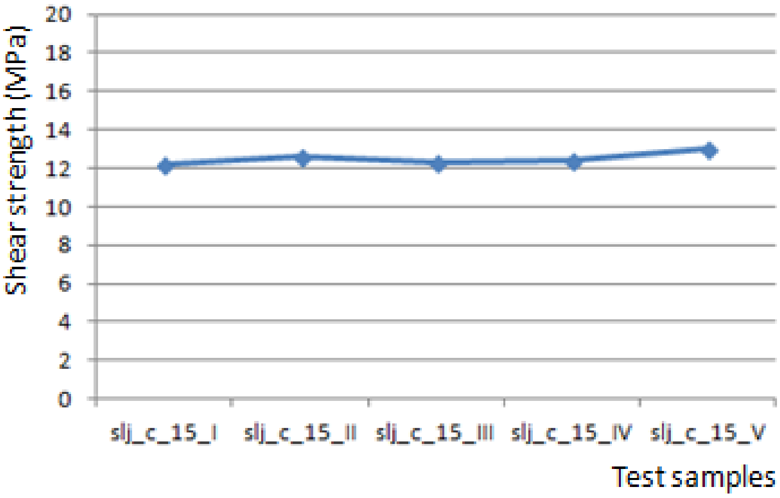

Figure 4.13: Graphical representation of slj_c_15 results.

4.2.3 Slj_c_30

Same as slj_c_0 we perform five experiments, and we named them like previous one. slj_c_30_I it means test sample one of 30 degree angle of carbon. And then goes like this way, slj_c_30_II, slj_c_30_III, slj_c_30_IV and slj_c_30_V. For the first experiment our result is 6,16 kN. Area is same. Sample I and II are shown in the Figure 4.14.

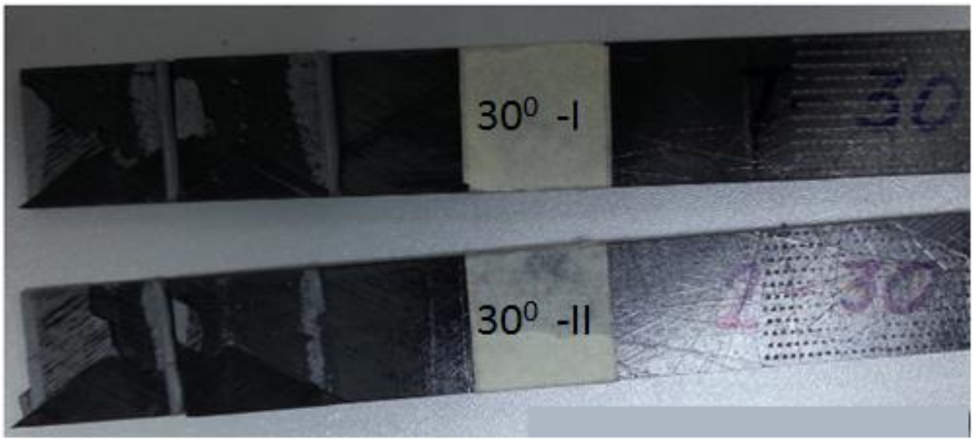

Figure 4.14: Test sample of slj_c_30_I and slj_c_30_II.

In this experiment we observed visually that adhesive is scattered around the lab and one layer of cured prepreg is broken away from the test part in the bonded area during breaking. View of part after breaking is shown in Figure 4.15.

Figure 4.15: View of test part after breaking.

We have finished the calculation of tensile lap shear strength of 30 degree samples. In the table 4.9 and Figure 4.16 below, we can find all of the results of 30 degree samples and graphical representation of results.

Table 4.9: Tensile lap shear strength of 30 degree samples.

30 degree sample numbers	τ (MPa)
slj_c_30_I	10,34
slj_c_30_II	10,18
slj_c_30_III	10,40
slj_c_30_IV	10,88
slj_c_30_V	10,11
slj_c_30	10,38 ±0,3

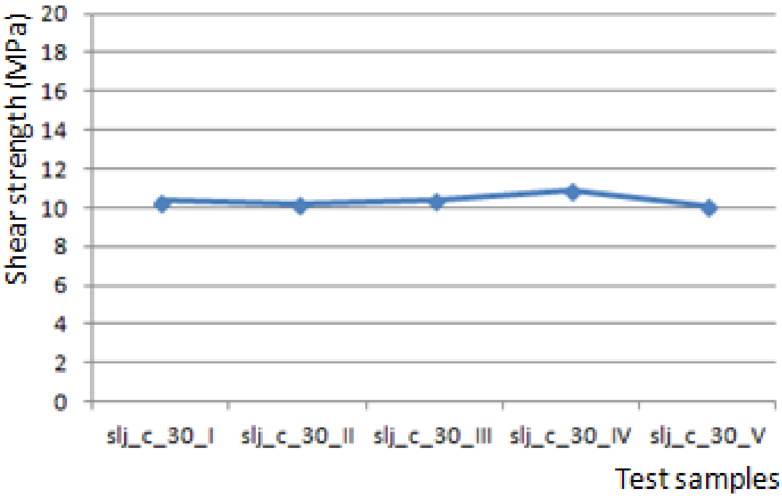

Figure 4.16: Graphical representation of slj_c_30 results.

4.2.4 Slj_c_45

Same as slj_c_0 we perform five experiments, and we named them like previous one. slj_c_45_I it means test sample one of 45 degree angle of carbon. And then goes like this way, slj_c_45_II, slj_c_45_III, slj_c_45_IV and slj_c_45_V. For the first experiment our result is 6,08 kN. Area is same. Sample I, II and III are shown in the Figure 4.17.

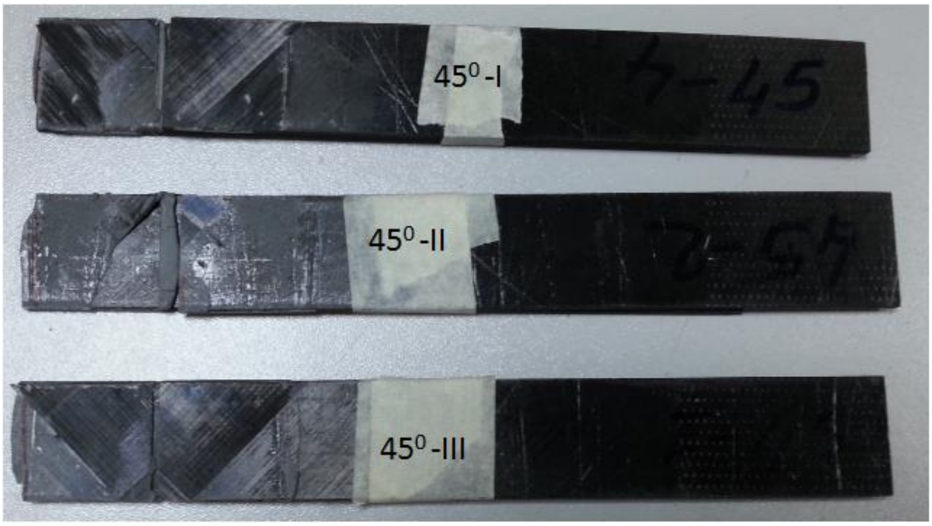

Figure 4.17: Test sample of slj_c_45_I, II and III.

In this experiment we observed visually that two layers of cured prepreg are broken away from the test part in the bonded area as shown in Figure 4.18. Cured adhesive is scattered around the lab.

Figure 4.18: Breaking away part in the bonded area.

We have finished the calculation of tensile lap shear strength of 45 degree samples. In the table 4.10 and Figure 4.19 below, we can find all of the results of 45 degree samples and graphical representation of results.

Table 4.10: Tensile lap shear strength of 45 degree samples.

45 degree sample numbers	τ (MPa)
slj_c_45_I	9,73
slj_c_45_II	9,66
slj_c_45_III	9,17
slj_c_45_IV	8,8
slj_c_45_V	9,68
slj_c_45	9,41 ±0,41

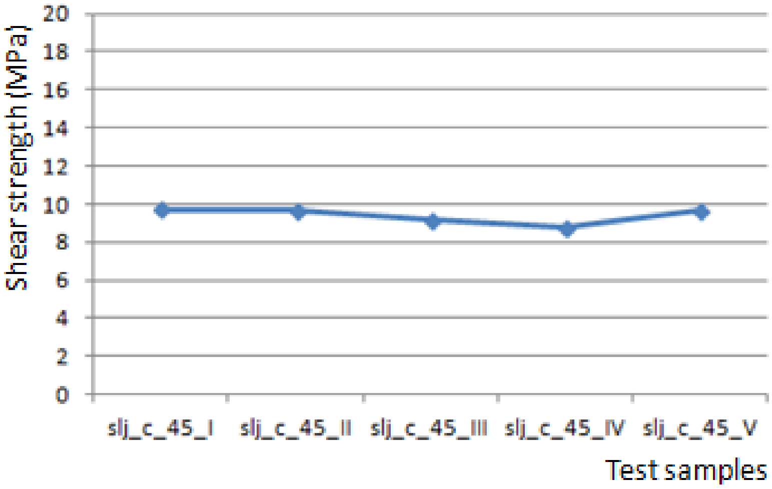

Figure 4.19: Graphical representation of slj_c_45 results.

4.2.5 Slj_c_60

Same as slj_c_0 we perform five experiments, and we named them like previous one. slj_c_60_I it means test sample one of 60 degree angle of carbon. And then goes like this way, slj_c_60_II, slj_c_60_III, slj_c_60_IV and slj_c_60_V. For the first experiment our result is 5,10 kN. Area is same. Sample I, II, III and IV are shown in the Figure 4.20.

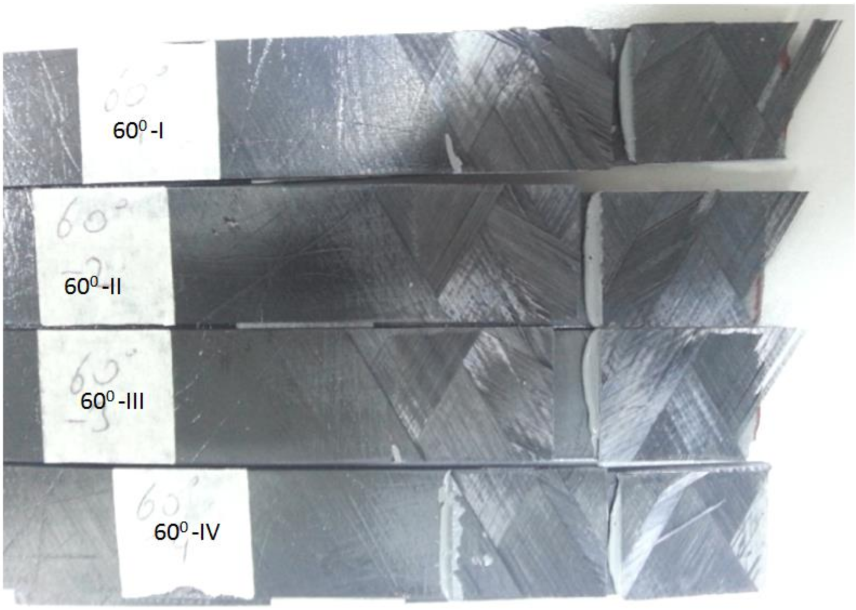

Figure 4.20: Test sample of slj_c_60_I, II, III and IV.

In this experiment we observed visually that three sometimes four layers of cured prepreg are broken away from the test part in the bonded area. Adhesive has been scattered around the lab again.

We have finished the calculation of tensile lap shear strength of 60 degree samples. In the table 4.11 and Figure 4.21 below, we can find all of the results of 60 degree samples and graphical representation of results.

Table 4.11: Tensile lap shear strength of 60 degree samples.

60 degree sample numbers	τ (MPa)
slj_c_60_I	8,16
slj_c_60_II	8,24
slj_c_60_III	8,11
slj_c_60_IV	8,03
slj_c_60_V	8,69
slj_c_60	8,25 ±0,24

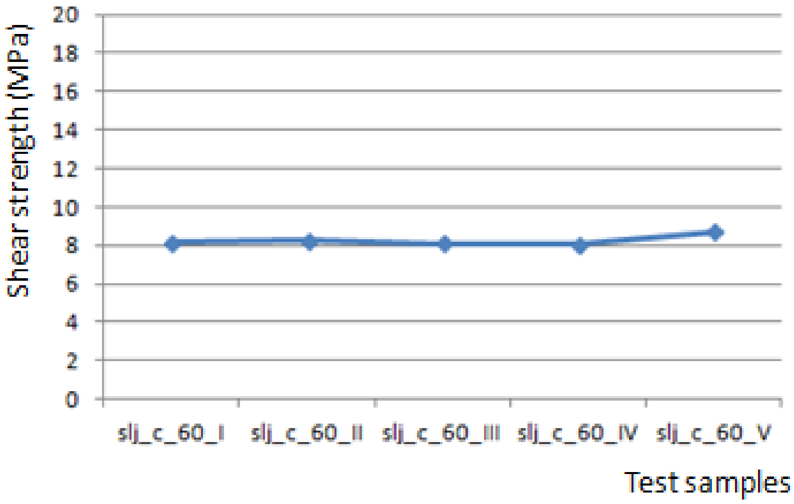

Figure 4.21: Graphical representation of slj_c_60 results.

4.2.6 Slj_c_75

Same as slj_c_0 we perform five experiments, and we named them like previous one. slj_c_75_I it means test sample one of 75 degree angle of carbon. Then, goes like this way, slj_c_75_II, slj_c_75_III, slj_c_75_IV and slj_c_75_V. Our first experiment has no result, because the test part is broken away while the test machine shows 2,14 kN. There is no deformation in the bonded area, just the part is broken. Area is same. Sample I and II are shown in the Figure 4.22.

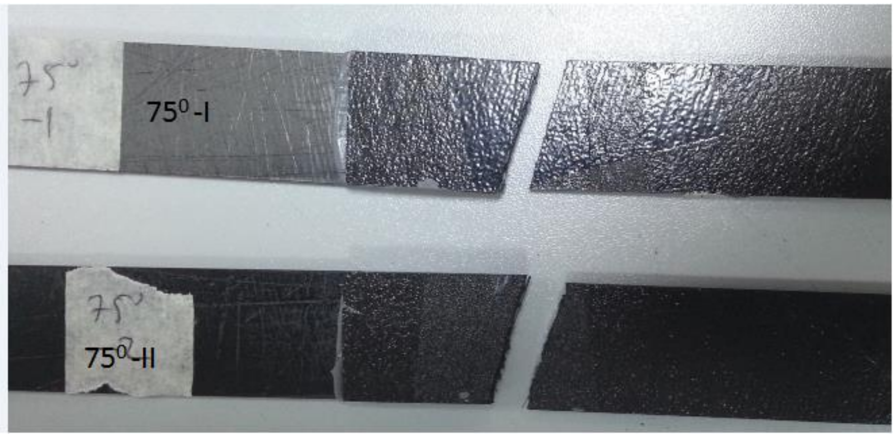

Figure 4.22: Test sample of slj_c_75_I and II.

Since the part is broken, we can list the values of breaking. Figure 4.23 below, gives the graphical representation of 75 degree results.

4.2.6.1 Slj_c_75_I

Breaking force value is 2,14 kN

4.2.6.2 Slj_c_75_II

Breaking force value is 2,21 kN

4.2.6.3 Slj_c_75_III

Breaking force value is 2,22 kN

4.2.6.4 Slj_c_75_IV

Breaking force value is 2,10 kN

4.2.6.5 Slj_c_75_V

Breaking force value is 2,17 kN

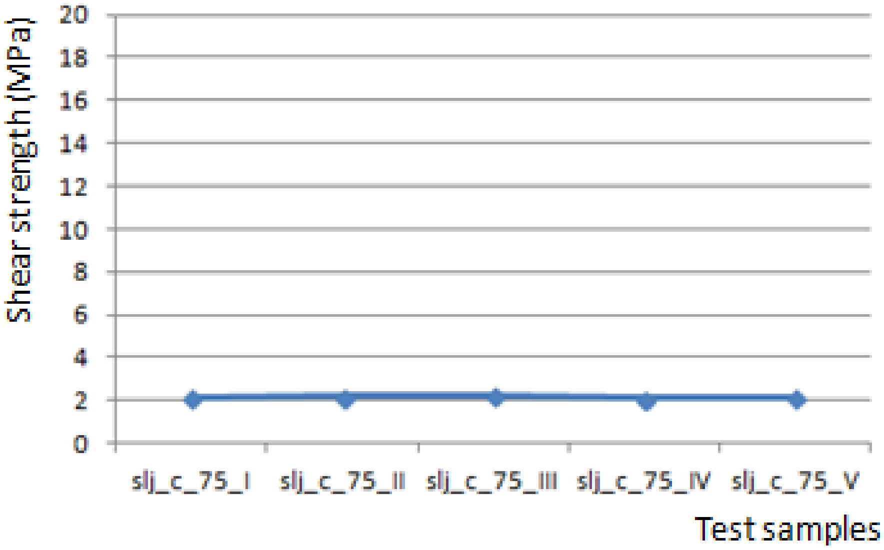

Figure 4.23: Graphical representation of slj_c_75 results.

Graphic representation of shear strength of bonded area is given below (Fig. 4.24). In the graph, since the bonded area is same the tangent of load vs. displacement is nearly same for all angle orientation.

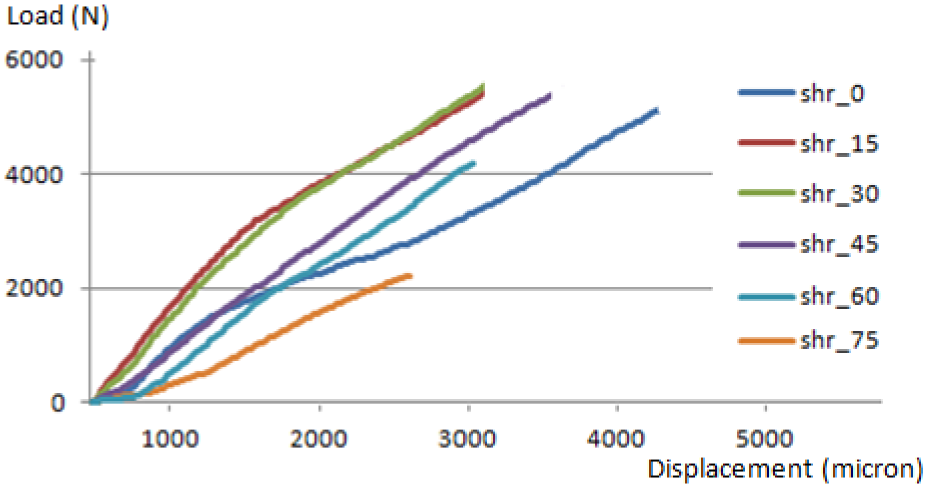

Figure 4.24: Graphic representation of load vs. displacement of shear test.

4.3 Flexural Strength (σ) of Carbon Fibres

Using eq. 3.1 we calculate the flexural strength of carbon fibres that we have been used in the test. The average results are given in the Figure 4.25.

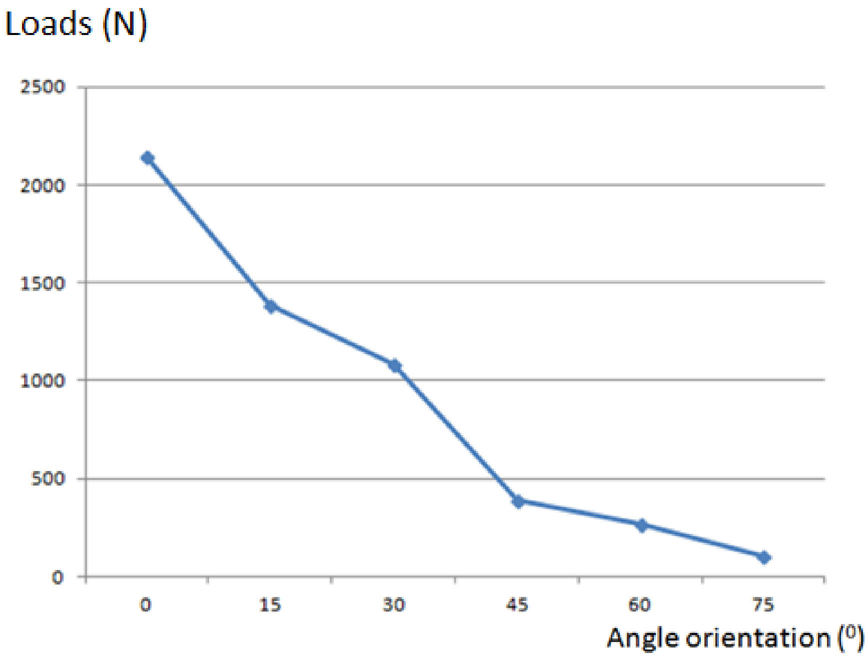

Figure 4.25: Graphic representation of load vs. angle orientation of carbon fiber.

It can be easily released that as the angle differs from 0, the load drastically decreases. At 0 degree the load is 2144 MPa, while at 75 degree the load is 108 MPa is calculated.

CHAPTER FIVE

DISCUSSION

As mentioned in the research objective section, the primary objective of this search is to observe the effect of different angle variation of carbon fiber reinforced composite on the performance of adhesively bonded joints. The results that will be discussed in this section help us to characterize angle variation of material.

This study was performed with two main goals. The first goal was to understand the properties of tape (Unidirectional prepreg) carbon fiber epoxy. For this purpose we have performed three point bending test. The second goal of this study was to observe the effect of different angle orientation of tape carbon fiber epoxy. Angle variations are 0^0, $\pm15^0$, $\pm30^0$, $\pm45^0$, $\pm60^0$ and $\pm75^0$. For this purpose we have performed tensile single lap shear strength.

In this thesis study, we have used ABS5139C1219/A (AIMS 05-01-001), carbon-epoxy prepreg, unidirectional, 196gsm, [14] as carbon–epoxy composite part and Hysol EA9394 two part adhesive [15] as adhesive.

After this study, elasticity modulus of carbon fiber epoxy and tensile strength of single lap joint will be discussed.

For 0 degree samples we have found the elasticity modulus 123,5 GPa; 125,4 GPa; 125,32 GPa; 124,2 GPa and 122,81GPa respectively. Average value is can be calculated as follows: (123,5 + 125,4 + 125,32 + 124,2 + 122,81) / 5 = 124,246 GPa.

In the material standard of AIMS 05-01-001 table 5.1 mechanical properties – dry (grade A, B, C) gives us the tensile modulus for 0 degree is 135 ±15 GPa. It means tensile modulus is between 120 and 150 GPa. Our elasticity modulus is in this range and consistent.

For ±15 degree samples our elasticity results were 101,44 GPa; 105,75 GPa; 104,44 GPa; 101,77 GPa and 102,90 GPa. Average value can be easily calculated as follows: (101,44 + 105,75 + 104,44 + 101,77 + 102,90) / 5 = 103,26 GPa. This result shows that elasticity modulus of 15 degree of carbon samples is decreasing since for 0 degree it was 124,246 GPa.

For ±30 degree samples our elasticity results were 59,14 GPa; 57,0 GPa; 58,91 GPa; 57,0 GPa and 56,99 GPa. Average value can be easily calculated as follows: (59,14 + 57,0 + 58,91 + 57,0 + 56,99) / 5 = 57,808 GPa. This result shows us that the elasticity modulus of 30 degree samples is decreasing drastically since for 0 degree it was 124,246 GPa and for 0 degree it was 103,26 GPa.

For ±45 degree samples our elasticity results were 19,02 GPa; 18,34 GPa; 18,92 GPa; 18,95 GPa and 18,33 GPa. Average value can be easily calculated as follows: (19,02 + 18,34 + 18,92 + 18,95 + 18,33) / 5 = 18,712 GPa. In this case decreasing is more drastically than previous ones.

For ±60 degree samples our elasticity results were 12,38 GPa; 12,53 GPa; 11,99 GPa; 12,28 GPa and 12,22 GPa. Average value can be easily calculated as follows: (12,38 + 12,53 + 11,99 + 12,28 + 12,22) / 5 = 12,28 GPa. It means that elasticity modulus of carbon fiber epoxy is getting smaller and smaller.

The most smallest elasticity modulus of carbon fiber epoxy is 75 degree samples since it is calculated as 9,274 GPa = (10,01 + 9,42 + 8,70 + 9,49 + 8,75) / 5.

Tensile lap shear strength of 0 degree samples is given table 4.7. These values are taken at 25^0C and %60 humidity. For five samples average value is 18,41 MPa that we have calculated from our results. The adherents are carbon-epoxy composite parts.

Bond strength performance is given in the document of manufacturer of Hysol EA9394 [15]. At the temperature of 25^0C it is 28,9 MPa. The adherents are 2024-T3 bare aluminum treated with phosphoric acid anodized. There is significant difference between them but the adherents are totally different. It is so difficult to lay up unidirectional prepreg to the moulding tool. There must be tolerance and our laying up operation is in this range. Preparing of bonding area is very important also. We prepared the surface carefully according to the manufacturer instruction stated in the document “Hysol® surface preparation guide”. Also it shows us that while designing adhesive bonding the type of adherents must be considered.

After this study we have realized that the performance of carbon fibre epoxy is negatively affected while changing the angle orientation. Our next study will be to observe the effect angle orientation while one layer is 0 degree, next one 90 degree and the others are ±45 degree. There will be totally twelve layer same as this study.

CHAPTER SIX

CONCLUSION

In this thesis study, effect of unidirectional carbon fibre angle orientation on the performance of adhesively bonded joints is investigated deeply. Fibre angles are 0^0, 15^0, 30^0, 45^0, 60^0 and 75^0 and each test sample part has 12 layers (prepreg). These parts are symmetric according to midline of the part.

First, we try to find the elasticity modulus (Young's Modulus) of carbon-epoxy parts. To do this, we use rectangular three point bending test. According to our results, elasticity modulus of 0 degree is higher than other angles. And then elasticity modulus of 15 degree samples comes. Ranking of elasticity modulus of angle orientation is 0 degree first, second one is 15 degree, third one is 30 degree, fourth one is 45 degree, fifth one is 60 degree and last one is 75 degree.

Secondly, we try to find the tensile lap shear strength of single lap joint. Same angle parts are used for this purpose. 0 degree has the biggest value. As the angle is further from 0, tensile lap shear strength value is getting smaller. Excluding 0 degree and 75 degree samples, since 75 degree samples are broken, breaking occurred at the bond area removing original plies from the test parts. Sometimes one ply, sometime four plies removed from the test parts are observed. These breaking parts scattered around the lab. While performing 75 degree samples, the test part is broken. No deformation on the bonded area observed. It shows that angle orientation of fibres must be considered while designing parts from composite materials.

The parts produced from 90 degree unidirectional fibres are broken into peaces while we are cutting them into the dimensions of test specimen. For this reason we could not perform the test for 90 degree angle orientation.

Not only angle orientation, but also cleaning of bonded surface, type of adhesive and curing condition of adhesive shall be thought for new design.

REFERENCES

1) T. Gerhard, C. Friedrich (2014). Mechanical fastening of carbon composite tubes, numerical calculation of axial loading capacity and experimental verification. *Composites:* Part B 67 391–399.

2) Till Vallee, Thomas Tannert , Rahul. Dimensioning method for bolted, adhesively bonded, and hybrid joints involving Fibre-Reinforced-Polymers. Meena, Simon Hehl. *Composites*: Part B 46 (2013) 179–187

3) P.P. Camanho, F.L. Matthews. Stress analysis and strength prediction of mechanically fastened joints in FRP: a review. *Composites*, Part A, Appl. Sci. Manuf. 28 (6) (1997) 529–547.

4) T.N. Chakherlou, M. Mirzajanzadeh, J. Vogwell, B. Abazadeha. Investigation of the fatigue life and crack growth in torque tightened bolted joints. *Aerosp. Sci. Technol.* 15 (2011) 304–313.

5) T.N. Chakherlou, H. Taghizadeh, A.B. Aghdam. Experimental and numerical comparison of cold expansion and interference fit methods in improving fatigue life of holed plate in double shear lap joints. *Aerosp. Sci. Technol*. 29 (2013) 351–362.

6) Zao Chen. *Pull through strength of bolted composite joints*. Master thesis. McGill University, Canada. March 2013.

7) C. Stocchi, P. Robinson, S.T. Pinho. A detailed finite element investigation of composite bolted joints with countersunk fasteners. *18TH international conference on composite materials.*

8) Jianfeng Li, Ying Yan, Taotao Zhang, Zudian Liang. Experimental study of adhesively bonded CFRP joints subjected to tensile loads. *International Journal of Adhesion & Adhesives* 57(2015)95–104

9) MD Banea and LFM da Silva. Adhesively bonded joints in composite materials: an overview. *J. Materials: Design and Applications*. 2009: Vol.223. 1-18.

10) Da Silva LFM, das Neves PJC, Adams RD, Spelt JK. Analytical models of adhesively bonded joints-Part I: literature survey. *Int J Adhes Adhes* 2009;29: 319–330.

11) Walter Brockmann, Paul Ludwig Geiß, Jürgen Klingen, and Bernhard Schröder. *Adhesive bonding: materials, applications and technology*.

12]) Kelly A. Bond inspection in composite structures, In:, Zweben C, editors. *Comprehensive composite materials*. Oxford: Pergamon; 2000. p.359–392.

13) David K. HSU. Nondestructive Inspection of Composite Structures: Methods and Practice. *17th World Conference on Nondestructive Testing*, 2008, Shanghai, China.

14) Hart-Smith LJ. Bonded-bolted composite joints. *J Aircraft* 1985; 22 (11):993–1000.

15) Kelly G. Load-transfer in hybrid (bonded/bolted) composite single-lap joints. *Compos Struct* 2005; 69 (1):35–43

16) Kobye Bodjona, Larry Lessard. Load sharing in single-lap bonded/bolted composite joints. Part II: Global sensitivity analysis.

17) Fu M, Mallick P. Fatigue of hybrid (adhesive/bolted) joints in SRIM composites. *International Journal of Adhesion and Adhesives* 2001; 21 (2): 145–159.

18) Kelly G. Quasi-static strength and fatigue life of hybrid (bonded/bolted) composite single-lap joints. *Compos Struct* 2006; 72 (1):119–129.

19) Matsuzaki R, Shibata M, Todoroki A. Improving performance of GFRP/ aluminum single lap joints using bolted/co-cured hybrid method. *Compos* Part A 2008; 39(2):154–163.

20) Kweon J, Jung J, Kim T, Choi J, Kim D. Failure of carbon composite-to-aluminum joints with combined mechanical fastening and adhesive bonding. *Compos Structure* 2006;75(1):192–198.

21) FAA. *Advanced Composite Materials*, Chapter 7.

22) Ronald F. Gibson (1994). *Principles Of Composite Materials Mechanics*. New York: McGrew-Hill, Inc.

23) Johan Ekh. *Multi-Fastener Single-lap Joints in Composite Structures*. Doctoral Thesis in Lightweight Structures. ISBN 91-7178-396-2.

24) *Structures and materials*. NASA

25) Autar K. Kaw (2006). *Mechanics Of Composite Materials,* 2nd edition. New York: Taylor & Francois Group.

26) P.C. Pandey. *Composite materials*.

27) Douglas S. Cairns (). *Composite Materials For Aerospace Structures,*

28) Richard E. Ricker, Edward Escalante, and Mark R. Stoudt. Environmental effects on polymer matrix composites. *Tri-Service Conference on Corrosion*. M. Levy edt., Plymouth MA, 1992, US Dept. of Defense, pps 469-477.

29) Kalidass R., Balaji S. Tensile Test for Environmental Effect on Glass Fiber Composite Materials. *The International Journal of Engineering and Science* (IJES). 2014. Volume 3, Issue 1, Pages 23-27.

30) Waruna P. Seneviratne, and John S. Tomblin. Environmental Compensation Factor Influence on Composite Design and Certification. National Institute for Aviation Research, Wichita State University, Wichita, KS 67260-0093.

31) Shakila Umair. *Environmental Impacts of Fiber Composite Materials, Study on Life Cycle Assessment of Materials used for Ship Superstructure*. Master Thesis: Environmental Strategies Research. Stockholm, 2006.

32) M. B. Ruggles-Wrenn. Effects of Temperature and Environment on Mechanical Properties of Two Continuous Carbon-Fiber Automotive Structural Composites. *Metals and Ceramics Division*. 2003

33) Frederick T. Wallenberger, James C. Watson, and Hong Li. *Glass fibers*.

34) K.L. Loewenstein. The manufacturing technology of continuous glass fibers. Elsevier, 1993

35) www.camelyaf.com

36) Shahzad Alam, Farzana Habib, Muhammad İrfan, Waqas İqbal and Khuram Khalid. Effect of orientation of glass fiber on mechanical properties of GRP composites. *J. Chem.Soc.Pak.*, Vol. 32, No. 3, 2010

37) www.dupont.com

38) Karl K. Chang, E.I. *ASM handbook, volume 21, composites, Aramid fibers*. Du Pont de Nemours & Company, Inc

39) http://pslc.ws/macrog/aramid.htm

40) www.cytec.com

41) http://composite.about.com

42) Paul J. Walsh. *ASM handbook, volume 21, composites, Carbon fibers*. Zoltek Corporation

43) http://www.arrhenius.ucsd.edu/miakel/Miakel_B.html

44) Carbon fibre reinforced epoxy prepreg unidirectional 180^0C – curing class, standard modulus fibre, structural material

45) Hysol® EA 9394

46) Standard test method for flexural properties of unreinforced and reinforced plastics and electrical insulating material: ASTM D792

47) Standard test method for tensile properties of polymer matrix composite materials: ASTM D3039

48) Loctite aerospace, *Hysol® Surface Preparation Guide.* Loctite corporation.

49) www.floorsandingabrasive.com

50) www.testresources.net

51) Example1.

52) Ferdinand P. Beer, E. Russell Johnston, Jr., John T. Dewolf, David F. Mazurek (2012). *Mechanics of materials*, 6th edition. New York: McGrew-Hill, Inc.

53) Kris Cabral, Emily Boster, 2010. *Mechanical Testing Of Structural And Hybrid Epoxies*. Texas A&M University Department of Physics and Astronomy.

APPENDICES

Appendix-A: Ply Orientation Tables are Given Below For Each Test Specimen ....

Appendix-B: In This Section, Detailed Calculations of 0 Degree Sample is Given ....

Appendix-C: Here, Detailed Calculations Of Tensile Lap Shear Strength of Single Lap Joints of Carbon Fibre are Given ....

Appendix-A: Ply Orientation Tables are Given Below For Each Test Specimen

Table A.1: Ply orientation 0^0.

Ply number	Ply angle	Ply material
1	0	UD Carbon fiber/epoxy
2	0	
3	0	
4	0	
5	0	
6	0	
7	0	
8	0	
9	0	
10	0	
11	0	
12	0	

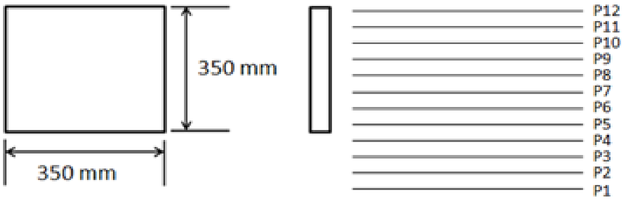

Table A.2: Ply orientation 15^0

Ply number	Ply angle	Ply material
1	+15	UD Carbon fiber/epoxy
2	-15	
3	+15	
4	-15	
5	+15	
6	-15	
7	-15	
8	+15	
9	-15	
10	+15	
11	-15	
12	+15	

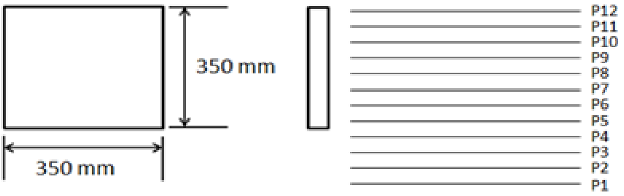

Table A.3: Ply orientation 30^0.

Ply number	Ply angle	Ply material
1	+30	UD Carbon fiber/epoxy
2	-30	
3	+30	
4	-30	
5	+30	
6	-30	
7	-30	
8	+30	
9	-30	
10	+30	
11	-30	
12	+30	

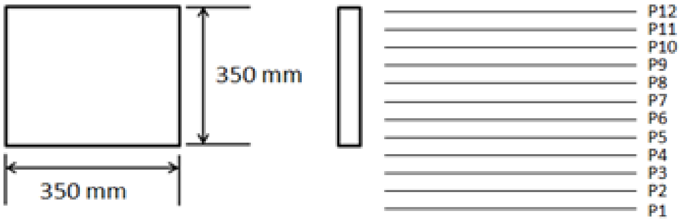

Table A.4: Ply orientation 45^0.

Ply number	Ply angle	Ply material
1	+45	UD Carbon fiber/epoxy
2	-45	
3	+45	
4	-45	
5	+45	
6	-45	
7	-45	
8	+45	
9	-45	
10	+45	
11	-45	
12	+45	

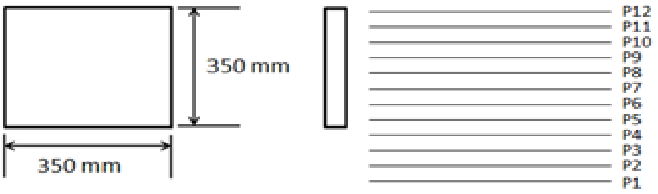

Table A.5: Ply orientation 60^0.

Ply number	Ply angle	Ply material
1	+60	UD Carbon fiber/epoxy
2	-60	
3	+60	
4	-60	
5	+60	
6	-60	
7	-60	
8	+60	
9	-60	
10	+60	
11	-60	
12	+60	

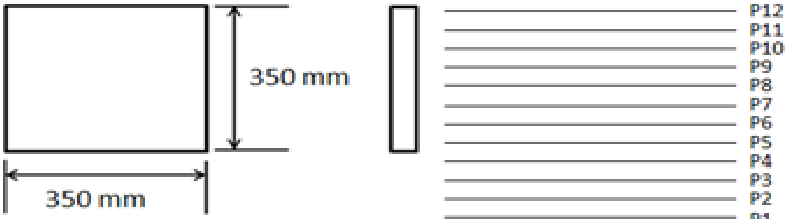

Table A.6: Ply orientation 75^0.

Ply number	Ply angle	Ply material
1	+75	UD Carbon fiber/epoxy
2	-75	
3	+75	
4	-75	
5	+75	
6	-75	
7	-75	
8	+75	
9	-75	
10	+75	
11	-75	
12	+75	

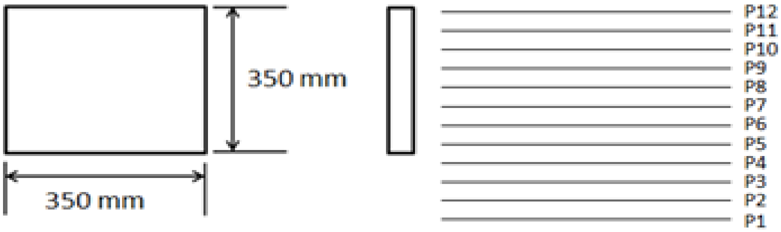

Table A.7: Ply orientation 90^0.

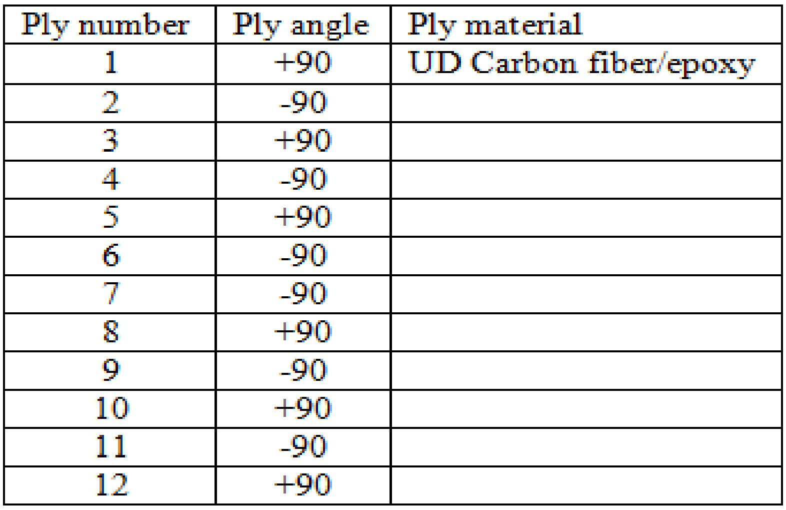

Ply number	Ply angle	Ply material
1	+90	UD Carbon fiber/epoxy
2	-90	
3	+90	
4	-90	
5	+90	
6	-90	
7	-90	
8	+90	
9	-90	
10	+90	
11	-90	
12	+90	

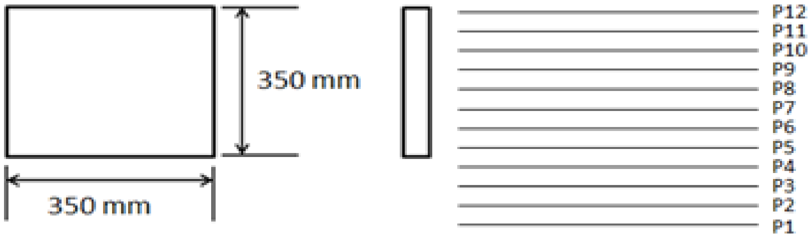

Appendix-B: In This Section, Detailed Calculations of 0 Degree Sample is Given

B.1 0 Degree Samples

Sample diameters of bnd_0_I are given in the Figure B.1. All dimensions are in mm.

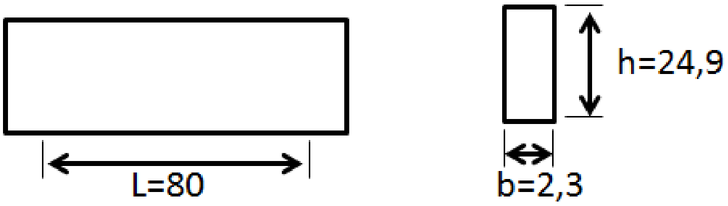

Figure B.1: Dimensions of bnd_0_I.

Now we define a procedure to calculate the Young's Modulus.

Step 1:

Gathering following experimental data

- Force (F) *
- Support length (L)
- Width of specimen (b)
- Height of specimen (h)
- Displacement (δ) *

* to calculate the average force and displacement choose first a force (F_0) value from experiment table, note the displacement (δ_0), then choose another force (F_1) value from same experiment table, note displacement again (δ_1). Subtract the values. This is our force value. With same method calculate the displacement.

$$F = F_1 - F_0 \qquad \textbf{Eq. 3.10}$$

$$\delta = \delta_1 - \delta_0 \qquad \textbf{Eq. 3.11}$$

Step 2:

Calculate polar moment of inertia (I) of rectangular specimen with the Eq.3.8

$$I_{rectangle} = (bh^3) / 12$$

Step 3:

Calculate Young's Modulus with the Eq.3.2

$$\delta = \frac{FL^3}{48EI} \text{ …Eq. 3.2 rearranging this for } E = \frac{FL^3}{48\delta I}$$

Now let's calculate our E for our bending test samples.

B.1.1 bnd_0_I

Step 1:

L=80 mm= 0,08 m

b= 2,3 mm = 0,0023 m

h= 24,9 mm = 0,0249 m

$F= F_1 – F_0 = 1058 \text{ N} – 444\text{N} = 614 \text{ N}$

$\delta = \delta_1 – \delta_0 = 4{,}215 \text{ mm} – 2{,}115 \text{ mm} = 2{,}1 \text{ mm}= 0{,}0021 \text{ m}$

Step 2:

Substitute these values in the Eq. 3.8 to calculate I;

$I = 25{,}25e^{-12} \text{ m}^4$

Step 3:

Use F, L, δ and I in the Eq. 3.2 to find the E:

$E= [614\text{N} * (0{,}08)^3] / [48 * (0{,}0021) * 25{,}25e^{-12}]$

E= 123,5 GPa

Appendix-C: Here, Detailed Calculations Of Tensile Lap Shear Strength of Single Lap Joints of Carbon Fibre are Given

C.1 slj_c_0_I

Let’s calculate bonded area.

$$A = 25 {*} e^{-3} {*} 25 {*} e^{-3} = 625e^{-6}\ \text{m}^2$$

$$F = 11{,}16\ \text{kN}$$

$$\tau = \frac{F}{A} \Rightarrow \tau = \frac{11160}{625e-6} = 17{,}856\ \text{MPa}$$

RESUME

PERSONNEL INFORMATION

Name Surname : Hasan PÜSKÜL
Place/Date of birth : Erdemli 1978
E-mail : hasanpuskul@gmail.com
Phone : +90 536 221 0588

EDUCATION

High school : Amasya Anatolian Teacher Training High School 1999
University : Middle East Technical University, Faculty of Education, Physics Education, MS. 2005

EXPERIENCE

2006- TUSAŞ. Ankara. Instructor (structure)

LANGUAGE

English